machines

MDPI

Article

Vulnerability Evaluation for a Smartphone Digital Twin Workshop under Temporal and Spatial Disruptions

Ding Zhang *, Yu Pei and Qiang Liu

Key Laboratory of Precision Electronic Manufacturing Technology and Equipment, Guangdong University of Technology, Guangzhou 510006, China

* Correspondence: dingzhang361@163.com; Tel.: +86-188-9847-0821

Abstract: Dynamic performance analysis is essential for production systems facing random disturbances. In this paper, a vulnerability evaluation approach is proposed for smartphone assembly production systems with finite buffers under a resilient system analytic frame. Firstly, four important vulnerability indicators, namely Terminal Time Delay (TTD), Terminal Time Window (TTW), Bottleneck Time Delay (BTD), and Bottleneck Time Window (BTW), are defined to expound temporal and spatial attributes caused by disruptive events. Then, a recursive derivation approach of the queuing network model is presented to obtain a state-transition matrix, wherein machine reliability is also considered in the model. Afterward, the exact solutions of steady and transient vulnerability are evaluated based on state probabilities inference. Finally, numerical studies are carried out to validate the proposed method and translate it into a practical tool. An application program with vulnerability analysis and disturbance control functions is developed, embedded in the digital twin system independently developed by our team to solve practical problems.

Keywords: smartphone production systems; digital twin; finite buffers; vulnerability analysis; temporal and spatial attributes; dynamics analysis

Citation: Zhang, D.; Pei, Y.; Liu, Q. Vulnerability Evaluation for a Smartphone Digital Twin Workshop under Temporal and Spatial Disruptions. *Machines* **2022**, *10*, 752. https://doi.org/10.3390/machines10090752

Academic Editors: Krzysztof Żywicki and Jose L. Martinez Lastra

Received: 20 July 2022
Accepted: 26 August 2022
Published: 31 August 2022

1. Introduction

The products of computer, communication, and consumer electronics are replaced quickly. As the main resource of equipment to complete the product manufacturing cycle, the production line has a direct impact on the quality, cost, and delivery cycle of the product. During the production process, due to the frequent switching of the production line configuration, the disturbance factors will cause the production of local stations to be disordered and propagate along the branch link to the main link. Therefore, to ensure the stability of production capacity under frequent changes in production lines and disturbances, the design of the assembly system must be flexible.

Serial structures with intermediate finite buffers are most widely adopted in production systems. Normally, workstations are allocated according to certain process routes, and buffers are allocated in consideration of their line balancing and antijamming ability. The intervention of buffers causes the fluctuation of system performance. Traditional output indicators, such as productivity, due-time performance, and other statistical indicators, are general and effective steady-state metrics during production system modeling [1]. However, in industrial production, disturbance factors frequently come from both inside (machine failures, scheduled maintenance, the fluctuation of working time, quality defaults, etc.) and outside (urgent orders, product changeover, process change, etc.). Transient-state performance evolution cannot be well-studied under the traditional performance evaluation frame. Thus, the dynamics analysis of the production system is essential to customized design and operation optimization. Random failures and small disruptions may result in a catastrophic risk to production systems in the current highly interconnected manufacturing environment [2,3]. Performance reduction under such disruption can be well described

as a vulnerability metric, which is also well explained in the resilient system research field [4–6]. Henry and Ramirez-Marquez [7] described the resilience of a generalized engineering system by depicting the performance transition process. Hosseini et al. [6] divided the entire process into three separate intervals, and three performance indicators are applied to match these three intervals, which are reliability, vulnerability, and recoverability, respectively. Such description and definition can also be adopted in the production system field. The resilient production system can be modeled as a discrete event dynamics system. As a constituent part of system dynamic performance, vulnerability under disruptions is an important performance indicator in production system engineering. To some content, the vulnerability effect is ubiquitous in both production systems at the workshop level [8,9] and inter-enterprises supply chains [10]. Vulnerability risks include high maintenance/servicing costs, yield reduction, and more importantly, system outage and the final large-scale delivery delay.

System vulnerability analysis (SVA) is less studied in comparison with system reliability analysis (SRA) in the production system field. System reliability is the performance metric of a resilient production system (as shown in the first interval of Figure 1), which represents the continuous working ability without failures from the static perspective. However, SVA provides a quantification study in terms of failure effect analysis, with emphasis on the effect propagation of cascading failures. Studies on SRA provide a global steady-state performance metric for fulfilling specified functions on the macro level. Accordingly, SVA affords a local dynamics survey of disturbance influences. Equal attention should be paid to SRA and SVA for resilient production systems.

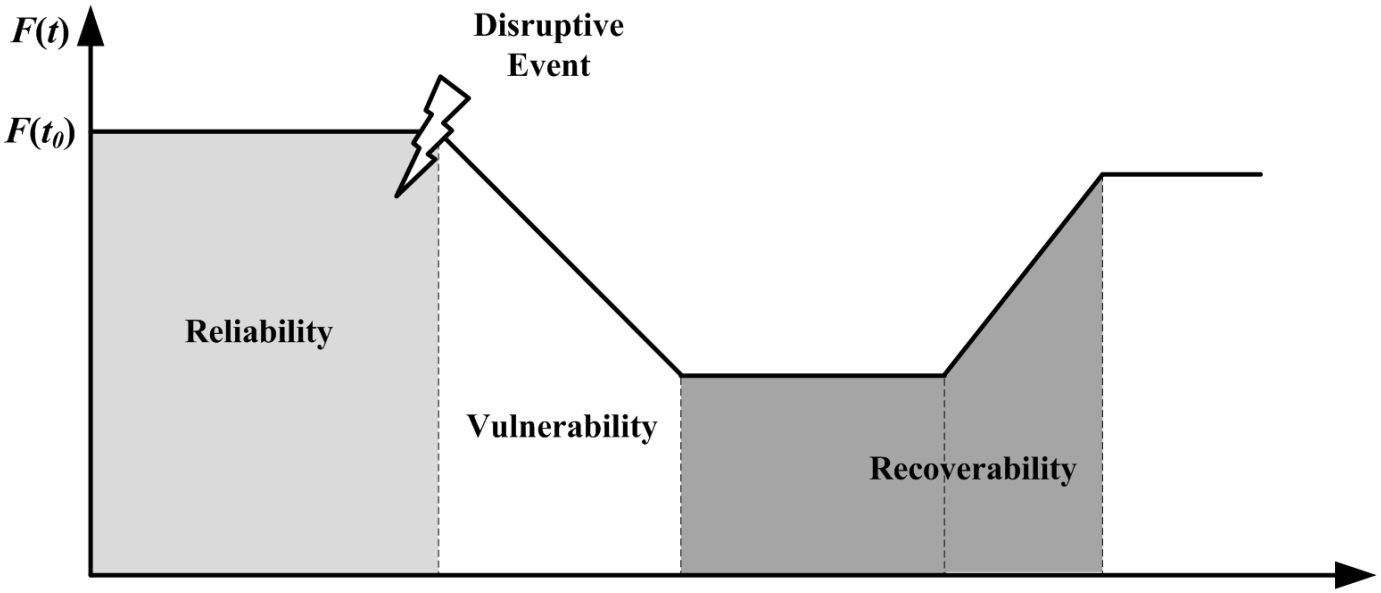

Figure 1. Performance transition of a resilient system.

For a reconfigurable electronic assembly line that is frequently replaced, it will take a lot of time to design a balanced production line structure, deploy tools, and debug and test after each disturbance causes system interruption. The digital twin platform of the production line can provide a virtual test optimization platform [11,12]. The data between the physical and virtual entities support each other in decision making, which is applied to the design, analysis, and regulation of the production line [13–15]. As the theoretical core of the extended application of digital twin technology, SVA plays a vital role in the evaluation and analysis module of the digital twin system. SVA provides the evaluation measures in the configuration and designing stage of production systems. Additionally, it is the fundamental work for performance control in the operational stage. New quantitative analysis methods and means should be developed to understand the nature of the vulnera-

bility effect. Vulnerability quantification is undoubtedly more valuable than mainstream qualitative analysis. However, it is difficult to construct a precise mathematical model due to the dynamic properties of the vulnerability effect. In this paper, a transient and steady vulnerability analysis approach is proposed for a resilient serial production system considering both temporal and spatial attributes. This method establishes a mathematical analytical model for the performance evaluation module in the twin system, which not only effectively avoids the shortcoming that the simulation model takes a long time, but also can evaluate the brittle effect of the dynamic disturbance during the operation of the production line.

The remainder of this paper is organized as follows: related works are reviewed in Section 2, wherein the innovation and difference from the presented works are briefly emphasized. Section 3 provides a digital twin system and architecture. Section 4 presents the temporal and spatial attributes of SVA of production systems. Section 5 provides the transient and steady vulnerability quantitative approach for both terminal station and bottleneck station. A case study is applied to verify the proposed method in Section 6. The conclusion and an outlook outlining ideas for future research are presented in Section 7.

2. Literature Review

2.1. Resilient Production System

System resilience has been a new performance metric for a dynamic system with disruption. Resilience system modeling has been studied for engineering systems such as grid networks [16] and infrastructure systems [17,18]. A major area of resilience research related to production is on the supply chain network. Some valuable reviews can be seen in [19–21]. Most papers in this area focus on the risk management of supply chain disruptions, which are dedicated to elucidating the attributes of resilience in different scenarios instead of quantizing it [22,23]. There are a few quantitative analytic models. A Bayesian network model is constructed to quantify the supply chain resilience of sulfuric acid manufacturers [24]. Xu and Radhakrishnan [25] developed a multidimensional nonlinear model to capture the dynamics of the supplier–manufacturer network. At the factory level, the concept of a resilient manufacturing system was proposed by Zhang and Luttervelt [4], and related guidelines for design and management are also discussed for resilient manufacturing systems. Production loss, throughput settling time, and total under-production time are used to measure the resilience of the manufacturing system by Gu and Jin, and the proposed resilience metrics are applied to assist in the reconfiguration of system design [26]. The optimal control policy of operation rate to achieve resilience in a class of serial manufacturing networks is addressed under disruption [27]. In brief, the resilience mechanism is valuable to explore the dynamics principle under disruption, and quantitative evaluation for manufacturing systems with certain structures still needs to be further studied.

2.2. Vulnerability Analysis of Production System

Vulnerability is the dynamic performance index of the system under disturbance. The quantitative evaluation of vulnerability is the premise of disturbance control. In the field of production system manufacturing, SVA plays as the second procedure of a resilient system in Figure 1 which is also vital for the dynamics modeling of production systems. A systematic method to quantitatively study the vulnerability assessment of production systems has not been well developed to date. Compared with performance models of production quantity, some vulnerability models in terms of production quality control are proposed by applying network modeling or fuzzy theory. Qin and Zhao established a man–machine–environment brittleness model of dynamic quality characteristics using the brittleness theory of complex systems [28]. A fuzzy analytic hierarchy process is applied to further identify the brittle source of the complex manufacturing process [8]. Vulnerability value is measured for assembly manufacturing systems using complex network theory and simulation technology [9]. Alnino and Garavelli present a simple Markov model of a

just-in-time production system to identify the vulnerability of backorder probability [29]. Liu and Xv proposed a modeling and evaluation method for the structural vulnerability of manufacturing systems based on the universal generating function and information entropy principle [30]. Gao and Wang evaluated the structural vulnerability of reconfigurable manufacturing systems based on the entropy principle and Markov models [31].

A major research area of SVA is still on supply chain networks and their risk management, which center on network structure modeling and vulnerability source identification through node linking relation [10,32–34]. Nakatani et al. proposed a supply chain model using a directed graph based on life cycle inventory data, and the Herfindahl–Hirschman index is used to rank vulnerability indicators of disruption risks [10]. Petri-Net-based visualization and triangularization clustering algorithms are studied to offer insights into a supply chain vulnerability in [33]. Risk management to reduce production system vulnerability is discussed in [35,36]. In brief, the vulnerability evaluating model under dynamic disruption remains unexplored for structured systems in the production capacity perspective.

2.3. Transient Performance Analysis

In production systems engineering, a great deal of work has been devoted to analyzing the performance of manufacturing systems. Traditionally, production system modeling methods are limited to steady-state analysis [37–39]. Meerkov and Zhang explored transients of the states and outputs in serial production lines with Bernoulli machines [40]. Analytical formulas for evaluating the settling time of productivity rate and WIP using the Bernoulli Reliability Model are also provided by Ju et al. [41]. Hou et al. proposed a novel "split-view" method for transient and steady-state performance analysis of inhomogeneous assembly systems [42]. A Production line with a rework loop is further studied using a "self-view" method from a buffer's viewpoint [43]. Based on Markov analysis, Chen and Huang proposed an auxiliary production line to decouple the dynamics of the original system to study the transient behavior of the production line [44]. Jia and Chen studied the transient performance evaluation problem by considering adjustments and resets on serial production lines for multi-type and low-volume production [45]. Huang and Wang introduced an analytical model to study the transient performance of a multi-product serial production line with Bernoulli reliability machines and non-negligible settings during changeover [46]. In brief, these mentioned approaches are centered on transient-state performance evaluation before reaching the steady state, for example, the typical warming-up period and shift transferring period [47]. However, transient performance analysis under sudden disruptions, such as random machine failures and other scheduled shutdowns (e.g., preventive maintenance activities), is less popularly studied and needs to be further explored.

In the related research on performance evaluation, most research literature focuses on evaluating the steady-state performance of manufacturing systems and analyzing the performance indicators of the system under long-term operation. The study of transient performance of manufacturing systems also mainly focuses on evaluating the performance of the system before reaching a steady state. Additionally, studies on how perturbation events will affect system state and capacity are rare. In the related research on vulnerability, most of the research objects are various complex systems. All of them have only carried out qualitative analysis on vulnerability, and there are few quantitative studies on system vulnerability. In practice, the impact of disturbance events on system performance is not immediately apparent due to the presence of buffers in manufacturing systems. There is even a time window in which system productivity is not affected, but little research has been conducted on this.

Therefore, the current research on the vulnerability of manufacturing systems is still insufficient, and it is necessary to pay attention to the impact of disturbance events on system productivity, quantify the capacity loss and opportunity time window, and then formulate the control strategy of the production line under disturbance. Based on the previous research results, this paper has made certain innovations on its basis:

The essence of the dynamic analysis of production systems is mainly discussed, and an evaluation method of production line vulnerability under the framework of elastic system analysis is proposed.

The method can perform transient performance analysis in the face of the sudden random disturbance production system. By quantitatively evaluating the vulnerability index of the production line under disturbance events, and formulating the regulation strategy under disturbance based on the vulnerability time window, the production loss caused by disturbance can be avoided or reduced.

The mathematical analysis model established by this method was successfully applied to the performance evaluation module in the digital twin system of the mobile phone production line developed by our team, and the research results of this paper were transformed into tools that can solve practical production problems.

3. Digital Twin System and Architecture

3.1. Digital Twin System

The assembly process of smartphones is very complex and involves many processes, including five main process steps: soldering, assembling, inspecting, quality control, and marking. For a reconfigurable electronic assembly line that is frequently replaced, it will take a lot of time to design a balanced production line structure, deploy tools, and debug and test after each disturbance causes system interruption. Therefore, in order to guarantee stable production capacity, the assembly line of the mobile phone manufacturing shop must be flexible, quickly reconfigurable, and adaptable to random interruptions.

As an emerging technology, the digital twin provides a new idea for the disturbance control and reconfiguration of mobile phone assembly lines. The digital twin system of the production line can provide a virtual test optimization platform. The data between the physical and virtual entities support each other in decision making, which is applied to the design, analysis, and regulation of the production line. As shown in Figure 2, a reconfigurable electronic assembly line digital twin system with disturbance analysis and control was independently developed by our team.

The assembly process of the smartphone can be divided into various processes such as sticking double-sided tape, dispensing, TP pressing, sticking accessories, back cover locking screws, and pasting accessories. Based on this assembly process, we construct corresponding digital virtual assembly lines and physical assembly lines. As shown in Figure 3, on the virtual platform, we built a standardized general platform (SGP) with complete functions and built a variety of special assembly machines based on this general platform. Such as locking screw machines, sticking accessories machines, TP double-sided adhesive machines, etc., for mobile phone processing. At the same time, drag-and-drop autonomous guided vehicles (AGVs) are also built for loading and unloading machines. Figure 4 shows the physical assembly line of a smartphone and its components, each of which corresponds to the components of a virtual assembly line. Based on digital twin technology, two-way real mapping and real-time interaction between physical production lines and virtual production lines can be realized.

The digital twin system shown in Figure 2 is mainly divided into three parts, including the device layer, the control network layer, and the execution system layer. The device layer includes physical production lines and virtual production lines. The control network layer includes instruction synchronization. The execution system layer includes the MES system, data analysis center, cell control system, and the SCADA system. The solid line represents the instruction channel, and the dashed line represents the information channel. Production instructions (such as scheduling scenarios or reconfiguration decisions) are issued by the global manufacturing execution system (MES) to the cell control systems, which are then passed on to machine instructions in the shop floor control network. At the same time, the supervisory control and data acquisition (SCADA) system obtains the field data and provides the field monitoring data and simulation data for the future decision making of MES.

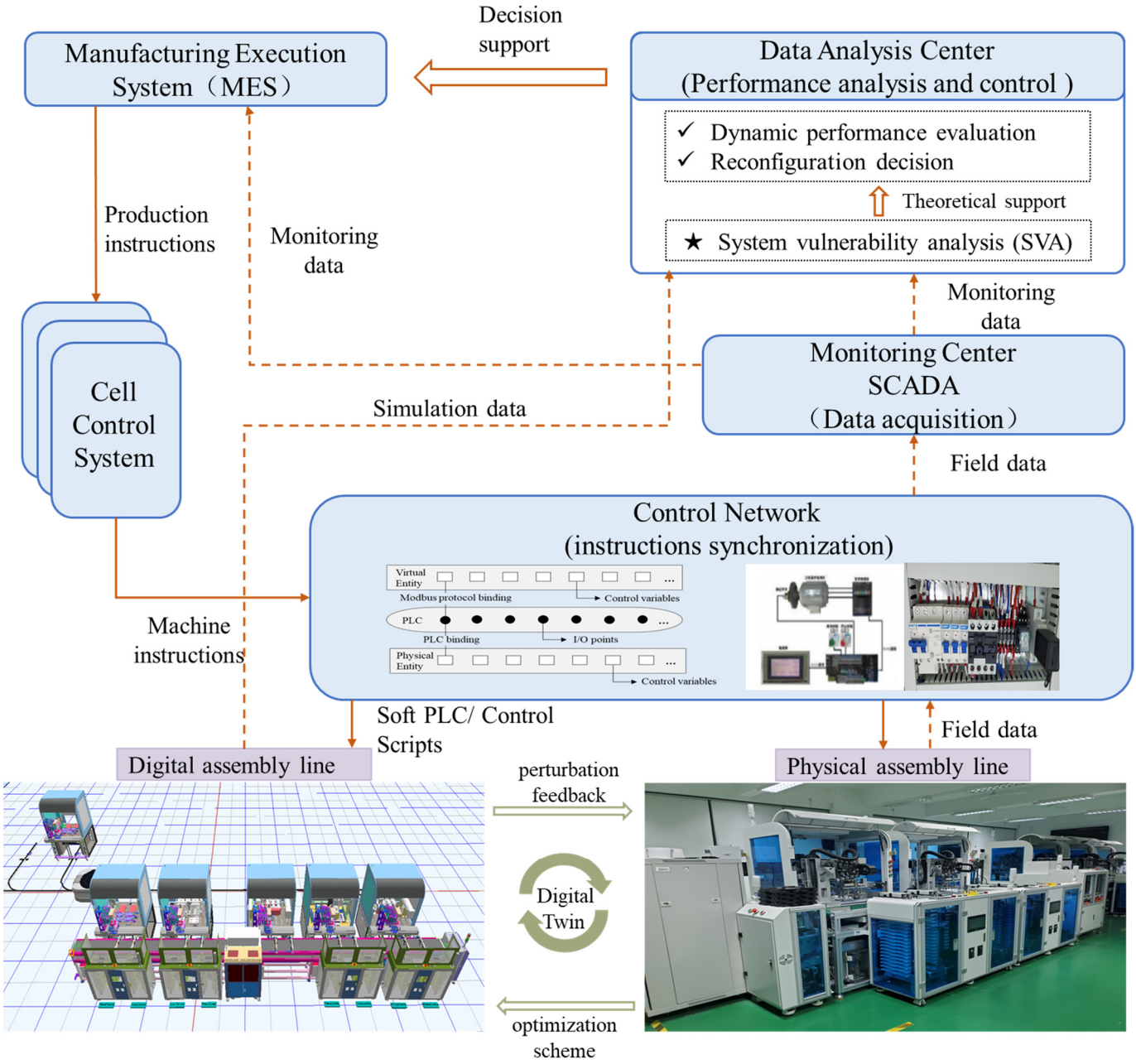

Figure 2. A digital twin system of disturbance evaluation and regulation.

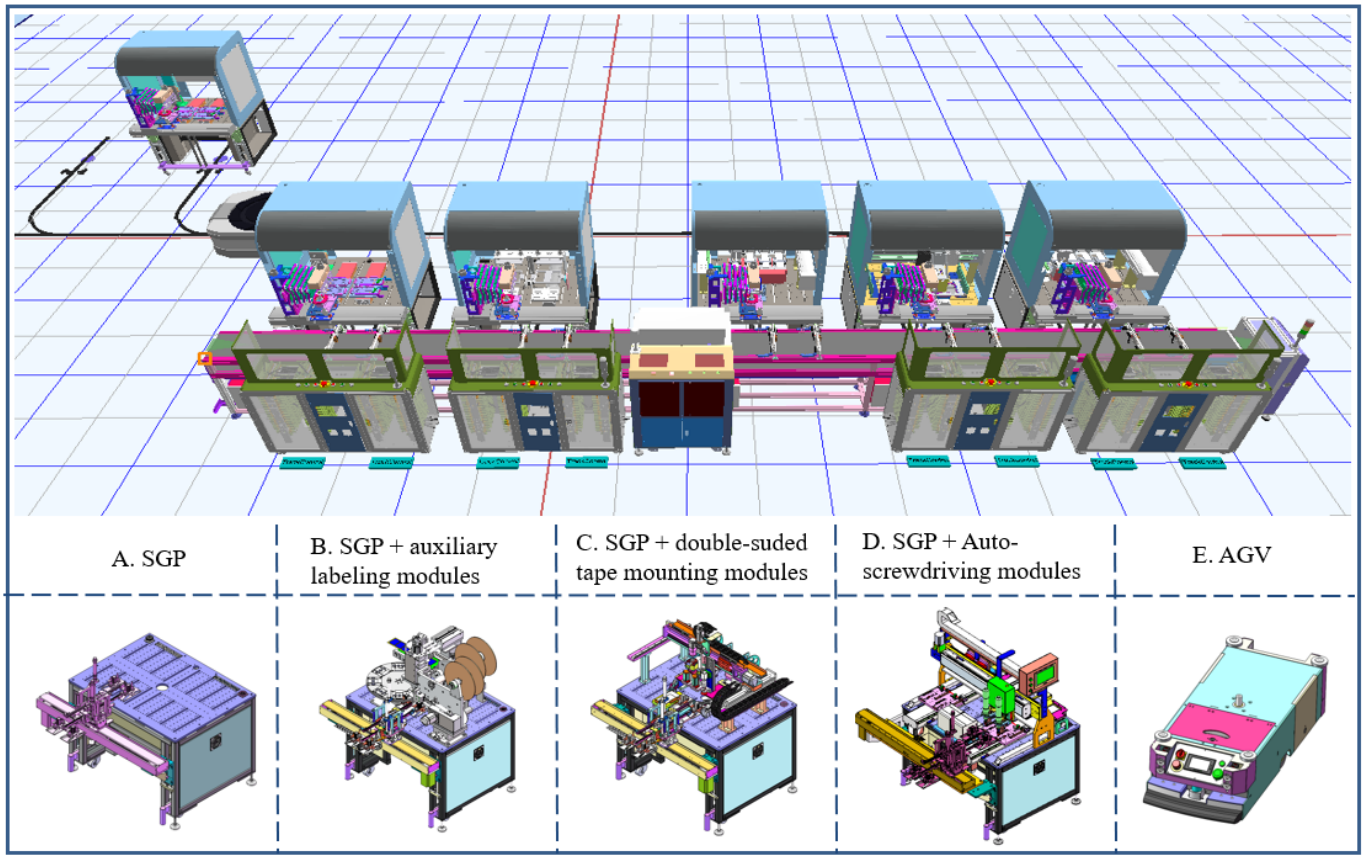

Figure 3. Virtual assembly line and its components.

For the digital twin system, a bidirectional connection channel is established in order to realize the synchronous operation of the physical production line and the virtual production line. As shown in Figure 2, a physical entity has a corresponding virtual entity. The PLCs in the various devices of the physical assembly line can perform input/output. These inputs/outputs are then associated with the various devices of the virtual assembly line through the soft PLC interface of the simulation software. This enables synchronization of physical and virtual production lines.

When the electronic assembly line is disturbed, the disturbance information is transmitted through the established bidirectional connection channel between the physical space and the information space, and the real-time state monitoring of the physical entity is reflected in the virtual model. The virtual model is used to simulate the line state evolution in advance, and the performance evaluation module of the data analysis center evaluates the influence of disturbance on the whole system's fault fluctuation. Then, the structure and performance of the production line can be regulated through optimization algorithms. Finally, the optimization plan and implementation measures are given to ensure the normal production output of the whole system.

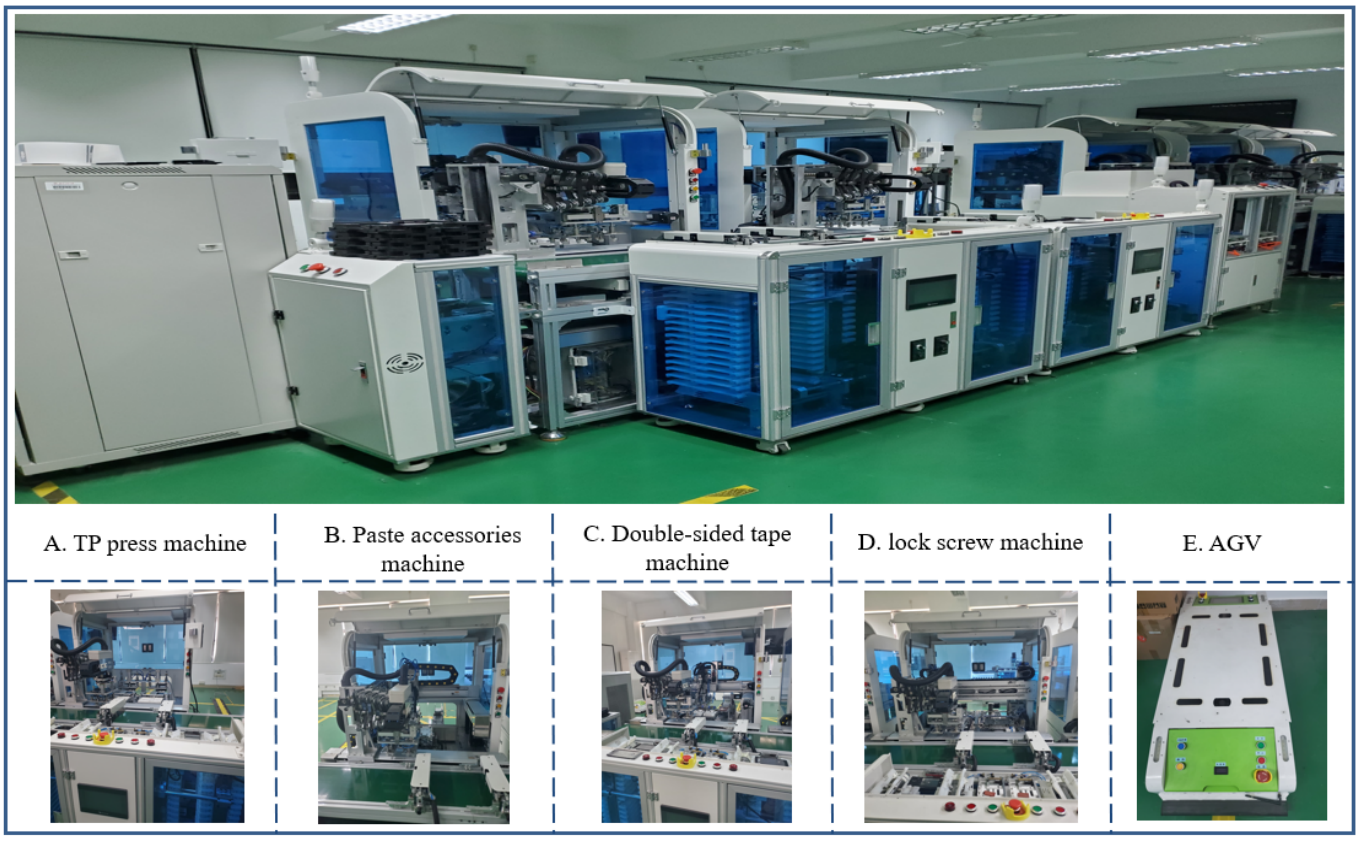

Figure 4. Physical assembly line and its components.

3.2. Notations and Assumptions

A digital twin system is far more than a virtual 3D model (visualization), and an accurate analytical model is essential to describe the internal operating mechanism of the system. The vulnerability analysis method proposed in this paper provides a theoretical core for the extended application of digital twin technology. As shown in Figure 5, this paper models the mobile phone assembly production system as a series system with finite buffers for analysis. The following notations are adopted in Abbreviations.

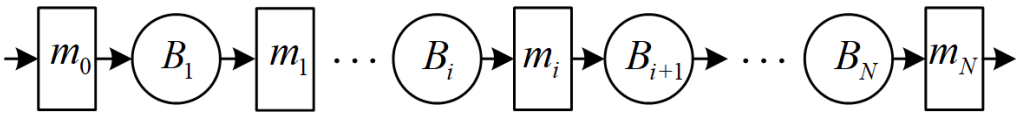

Figure 5. General system configuration structure.

The following assumptions are made in the process of SVA.

(1) The first station m_0 is never starved, and the last station m_N is never blocked.
(2) All stations are failure-dependent and buffers are reliable.
(3) Stations' servicing time without consideration of failures obeys the deterministic distribution.
(4) The servicing time is deterministically distributed when machine failure has not occurred.
(5) Station failure obeys the exponential distribution.
(6) Traveling time at buffers is negligible.

4. Temporal and Spatial Attributes of SVA

A resilient production system can be considered a dynamic space–time system. Finite buffers can suppress the stochastic disturbance effect and enhance product stability in the system. The consumption of work-in-process in buffers is accompanied by the alternation

of the station's starvation and blocking states. On the other hand, random failures and scheduled disruptions (e.g., preventive maintenance activities) of different stations result in differentiated production losses owing to their disturbance moment and duration. Hence, production disturbances (device failures, batch variation, process time delay, etc.) combined with inherent buffering mechanisms contribute to the dynamics of cell phone assembly systems. Consequently, system state evolution has distinct temporal and spatial attributes during the process of SVA. On account of different analysis perspectives, SVA and its quantification are separated into two parts in this section: vulnerability effect on the end-of-line station of the assembly line and vulnerability effect on the bottleneck station of the assembly line.

4.1. Vulnerability Effect on End-of-Line Station

System yield is computed by the production count of the end-of-line station. Any disruption of due-time performance may lead to product shortage and the irretrievable risk of delivery delay. Once stoppage occurs in an end-of-line station, the downstream industry chains are likely to be badly hit. Thus, it is necessary to analyze the vulnerability effect on the end-of-line station.

As shown in Figure 6, once a failure event of a certain station occurs for a serial transfer line with $N + 1$ stations and N buffers, it is unlikely for the failure event to immediately cause system performance reduction because of the function of finite buffers. System state evolution heavily depends on the configuration structure. The disturbance event immediately leads to local instability of a certain station, but it takes a propagation time to cause production reduction at the end-of-line station. Such a phenomenon is explained as Terminal Time Delay (TTD) effect in this paper. On the other hand, there is an opportunity window for the repair process such that the end-of-line station's production will not stop. The opportunity window is indicated as Terminal Time Window (TTW) below.

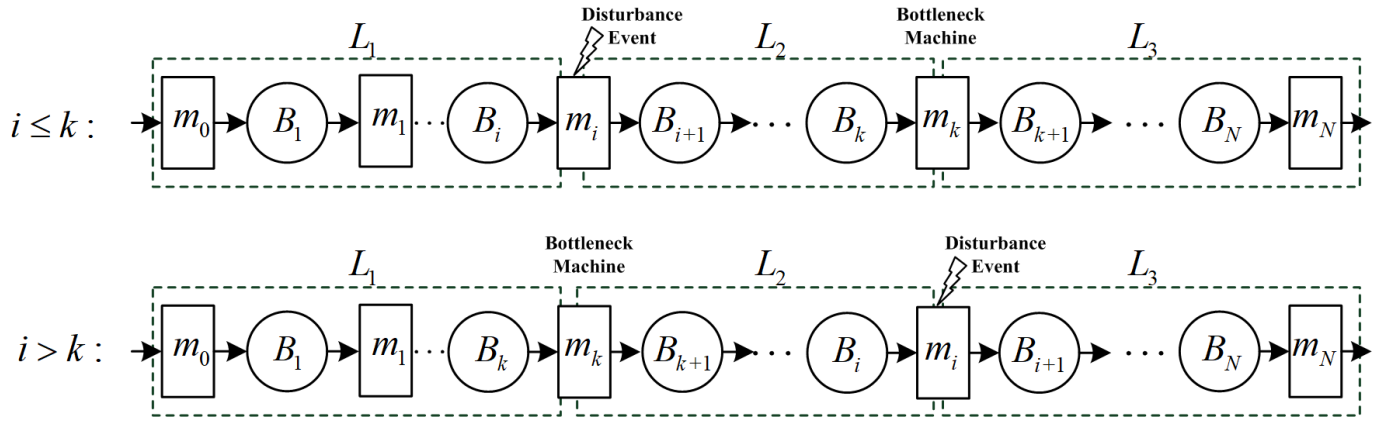

Figure 6. Line division according to the location of m_i and m_k.

Suppose a disturbance event E (m_i, t_e, d_e) occurs, wherein m_i is the i th station (i = 0, 1, 2, . . . , N), t_e is the occurrence time, and d_e is the duration of event E. The bottleneck station is indicated as m_k. The production system can be divided into three parts as Figure 5: line L_1 between the first station and m_i (m_k if m_i locates at the downstream of m_k, $I > k$), line L_2 between m_i and m_k, line L_3 between m_k (m_i if m_k locates at the upstream of m_i, $I > k$) and the last station.

TTD of the event $E(m_i, t_e, d_e)$, which is indicated as $TD_i(t_e)$, can be defined as follows.

Definition 1. *Terminal Time Delay (TTD) is the time interval between the occurrence moment of the disruption and the moment of production stoppage at the end-of-line station.*

As shown in Figures 7 and 8, the stagnant production of the end-of-line station does not occur until the time moment $t_e + TD_i(t_e)$. Accordingly, TTD can be represented qualitatively according to the residence time (RT) of line L_2 ($RT(L_2)$) and L_3 ($RT(L_3)$).

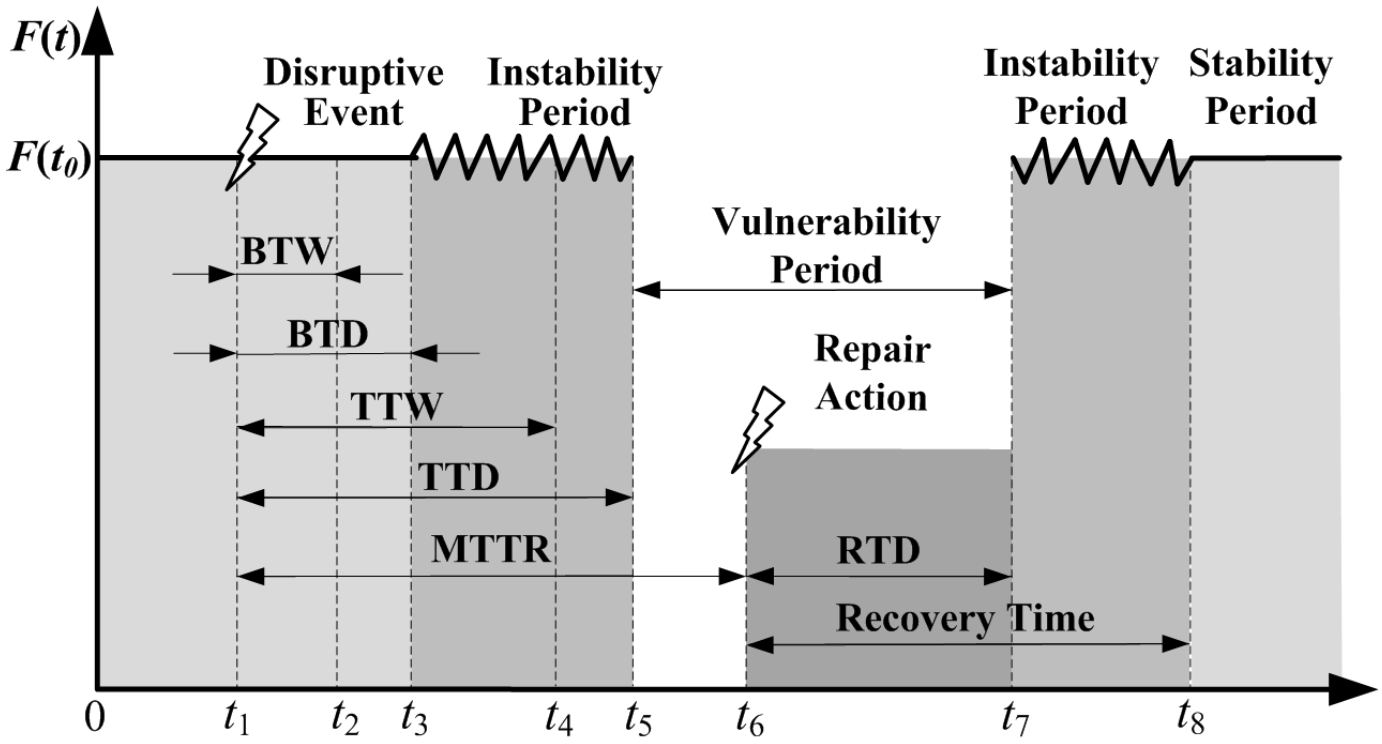

Figure 7. Description of temporal dynamics of a disruptive event ($i \leq k$).

As shown in Equation (1), TTD is determined in terms of the disruption location and occupancy situation of downstream buffers. Therefore, the disruption's TTD has a distinct spatial attribute determined by the distance from the last station. Additoinally, it also has distinct temporal attributes determined by the work-in-process (WIP) dynamics of downstream buffers and stations.

$$TD_i(t_e) = \begin{cases} RT(L_2) + RT(L_3) & i \leq k \\ RT(L_3) & i > k \end{cases} \quad (1)$$

The TTW of the event $E(m_i, t_e, d_e)$, which is indicated as $TW_i(t_e)$, can be defined as follows.

Definition 2. *Terminal Time Window (TTW) is the opportunity time that the disruption does not lead to the production stoppage at the end-of-line station.*

Note that the TTW is definitely less than the TTD. As shown in Figures 7 and 8, once the disturbance event $E(m_i, t_e, d_e)$ occurs, the last work-piece before disruption flows through line L_3 if $i > k$ (line L_2 and L_3 if $i \leq k$). There is an opportunity window for the repair process (the repair time is d_e) such that the first work-piece after repair catches up with the foregoing last work-piece exactly at m_N. Thus, m_N could never be stopped as if the disturbance event had never occurred.

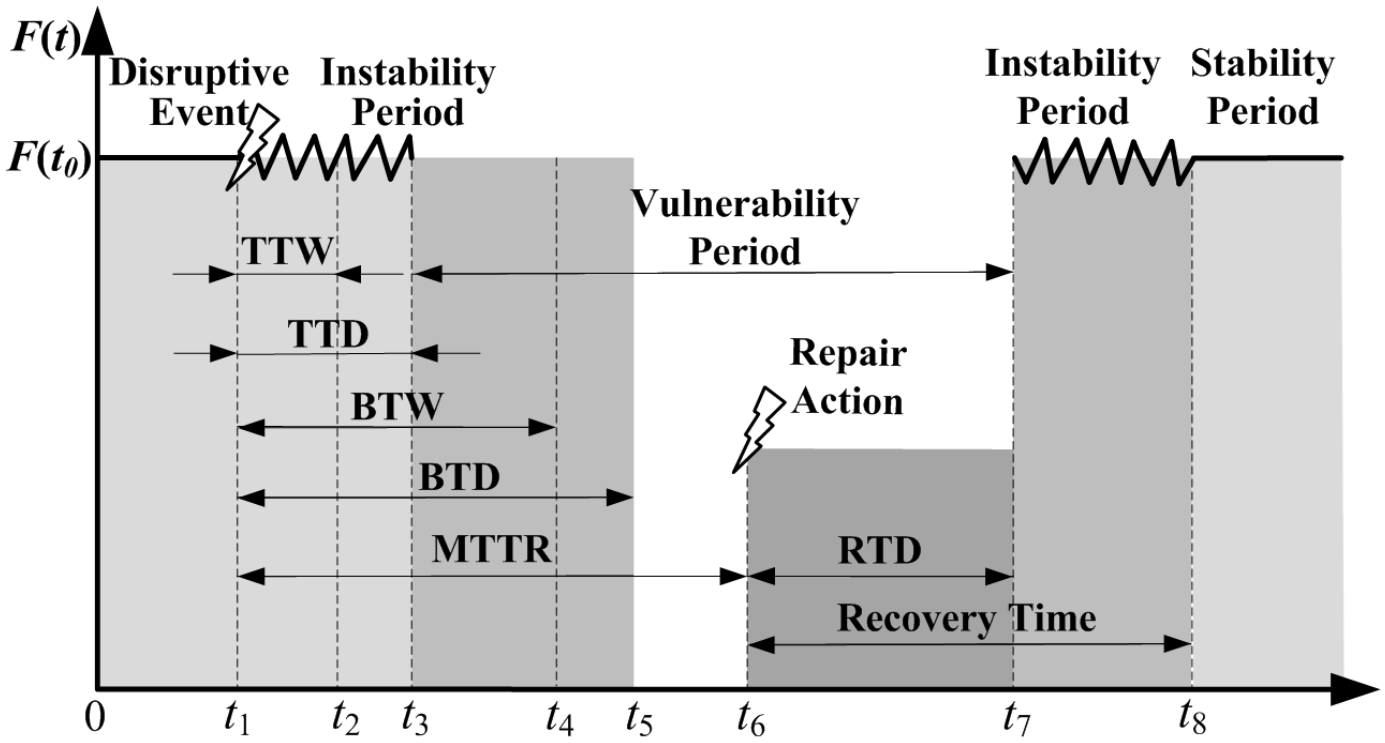

Figure 8. Description of temporal dynamics of a disruptive event ($i > k$).

Once $E(m_i, t_e, d_e)$ occurs, the vulnerability effect on the end-of-line station can be rescued if the following equation is satisfied.

$$TW_i(t_e) > d_e \tag{2}$$

If Equation (2) is not satisfied, production cessation at the end-of-line station will occur at $t_e + TD_i(t_e)$.

In conclusion, the values of TTD, TTW, and d_e jointly determine the triggering moment and effect of end-of-line vulnerability.

4.2. Vulnerability Effect on Bottleneck Station

According to the theory of constraints [48], system performance is restricted by the bottleneck station. Provided the bottleneck station m_k is not affected by the event $E(m_i, t_e, d_e)$, the production of the whole system remains stable owing to the buffering mechanism of line L_2. Namely, in the case of $i \leq k$, m_k keeps working because of the WIPs in line L_2; in the other case of $i > k$, m_k keeps working because of the vacancies in line L_2. Note that downtime of m_k will lead to permanent system production losses. Accordingly, $E(m_i, t_e, d_e)$ immediately leads to the local instability of neighboring stations of m_i, but it takes a certain duration of time for $E(m_i, t_e, d_e)$ to cause permanent system production losses. Such a duration of time is defined as Bottleneck Time Delay (BTD). On the other hand, there is an opportune time for the repair process such that the bottleneck station's production will not stop. The opportunity time is indicated as Bottleneck Time Window (BTW) below.

BTD of the event $E(m_i, t_e, d_e)$, which is indicated as $BD_i(t_e)$, can be defined as follows.

Definition 3. *Bottleneck Time Delay (BTD) is the time interval between the occurrence moment of the disruption and the moment of production stoppage at the bottleneck station.*

As shown in Figures 7 and 8, the stagnant production of the bottleneck station does not occur until the time moment $t_e + BD_i(t_e)$. Accordingly, BTD can be represented qualitatively according to the residence time (RT) of line L_2.

$$BD_i(t_e) = \begin{cases} RT(L_2) & i \leq k \\ RT\prime(L_2) - RT(L_2) & i > k \end{cases} \quad (3)$$

where $RT'(L_2)$ is the residence time of line L_2 when buffers between m_i and m_k are all full, $RT(L_2)$ is the normal mean residence time without the disruption.

BTD is determined based on the distance and buffer occupancy situation between m_i and m_k. Namely, if $i \leq k$, BTD is the time interval for all WIPs in line L_2 passing through m_k. If $i > k$, BTD is the time interval for all buffers in line L_2 becoming full. Therefore, the disruption's BTD has distinct spatial attributes determined by their distance. Additionally, it also has distinct temporal attributes determined by vacancy dynamics between m_i and m_k.

Definition 4. *Bottleneck Time Window (BTW) is the time interval between the occurrence moment of the disruption and the moment causing permanent production losses.*

Note that the BTW is definitely less than the BTD. As shown in Figure 7 ($i \leq k$), once the disturbance event $E(m_i, t_e, d_e)$ occurs, the last work-piece before disruption flows through line L_2. There is an opportunity window for the repair process (the repair time is d_e) such that the first work-piece after repair catches up with the foregoing last work-piece exactly at m_k. Thus, m_k could never be starved because of the disruption as if the disturbance event never occurs.

On the other hand, as shown in Figure 8 ($i > k$), once the disturbance event $E(m_i, t_e, d_e)$ occurs, there is an opportunity window for the repair process (the repair time is d_e), such that m_{k+1} returns to its normal work and obtains a work-piece from the full B_k. Thus, $E(m_i, t_e, d_e)$ will not lead to the blocking of m_k as if the disturbance event never occurs.

Let us construct such a scenario in the assumption of the continuous flow model [49]. The production line can be considered as a long rope with children (maybe on a mountaineering trip) tied in succession (similar to the Drum–Buffer–Rope model in the theory of constraints [48]). Once a child tumbles, there is a time window for his/her recovery that causes no effect on queue velocity. Thus, the time window is the time that ropes between the falling child and bottleneck child (maybe a 'little fatty') becoming totally tight if the falling child locates after the bottleneck child or becomes completely relaxed (children huddle together) if the bottleneck child locates after the falling child. The Drum–Buffer–Rope example is helpful for understanding the vulnerability delay. However, there is an error in such a continuous flow model. It holds that the bottleneck child will not be affected by the falling child as long as he/she recovers in the moments of the above two critical state limits. Jobs in mobile phone machining production lines are generally discretely delivered. Thus, it takes time to pass from the failure machine to the bottleneck machine.

Once $E(m_i, t_e, d_e)$ occurs, the vulnerability effect on the bottleneck station can be rescued if the following equation is satisfied.

$$BW_i(t_e) > d_e \quad (4)$$

If Equation (4) is not satisfied, permanent production losses of the entitled system will occur at $t_e + BD_i(t_e)$ because normal production of m_k is affected.

Similarly, the values of BTD, BTW, and d_e jointly determine the triggering moment and effect of bottleneck vulnerability.

As shown in Figure 6, once the disturbance event $E(m_i, t_e, d_e)$ occurs, the production process of the whole system remains stable during the time interval $[t_e, t_e + BD_i(t_e)]$. As shown in Figure 7, the production process of the whole system turns to be unstable because of the new bottleneck of line L_3, and such a period sustains at the time interval $[t_e, t_e + TD_i(t_e)]$. It is remarkable that there is no relationship of size between BTD and TTD

or BTW and TTW. In another way, BTW can be defined as the longest possible downtime of m_i that does not result in permanent production loss at m_N. TTW can be defined as the longest possible downtime of m_i that does not result in the production stoppage of m_N.

As shown in Figures 7 and 8, the time span between a disruptive event and the repair action can be quantified as mean time to repair (MTTR), which is indicated as d_e in this paper. Similarly, there is Recovery Time Delay (RTD) for productivity restoration because of the existence of propagation time. Furthermore, a longer period is consumed to recover to a stable state.

5. Vulnerability Quantification

Equations (1)–(4) give qualitative descriptions of the vulnerability effect on the end-of-line station and bottleneck station of the mobile phone assembly line. However, system vulnerability should be further quantified in the following procedures. We can consider the mobile phone production system in Figure 6 as a tandem open queuing network system. Thus, production performance can be estimated by the stochastic service system model.

5.1. Stochastic System Model

The transition probability matrix of the tandem system with $(N + 1)$ stations is deduced recursively in this subsection.

The servicing rate of m_i is indicated as a constant μ_i when failure is not considered. Failure time obeys exponential distribution with rate parameter λ_i. Suppose X_i and T_i are the producing number and survival time of m_i, respectively. Thus, we can infer the following equation.

$$\begin{aligned} P(X_i \le x_i) &= P(\mu_i T_i \le x_i) = P(T_i \le x_i/\mu_i) \\ &= \int_0^{\frac{x_i}{\mu_i}} \lambda_i e^{-\lambda_i x_i} dx_i = 1 - e^{-\frac{\lambda_i x_i}{\mu_i}} \end{aligned} \tag{5}$$

Therefore, if failures are considered, the servicing rate of m_i is an exponential distribution with parameter ω_i, which is calculated by:

$$\omega_i = \lambda_i/\mu_i, \qquad i = 0, 1, \ldots, N \tag{6}$$

Considering that the first station m_0 is never starved, the system can be modeled as an N node tandem open queuing network without m_0. Let $b_i(t)$ be the queue length at time t, $(i = 1, 2, \ldots, N)$. Thus, the state space is represented as $E_N = \{(b_2(t), b_1(t)\}$, which ranks in lexicographical order. The ith state-space E_i, which is i dimension Markov process, can be represented by E_{i-1} of the 1st to $(i - 1)$th service station.

$$E_i = \{(0, h), (1, h), \ldots, (B_i, h), h \in E_{i-1}\} \qquad 2 \le i \le N, E_1 = \{(0), (1), \ldots, (B_1)\} \tag{7}$$

In order to investigate the recurrence relation between E_{i-1} and E_i, the survey of a state-transition process for the first buffer B_1 is necessary. The birth and death rates are ω_0 and ω_1, respectively. The corresponding state-transition matrix Q_1 of E_1 is shown in Figure 9.

$$Q_1 = \begin{bmatrix} -\omega_0 & \omega_0 & & & & & \\ \omega_1 & -(\omega_0+\omega_1) & \omega_0 & & & & \\ & \omega_1 & -(\omega_0+\omega_1) & \omega_0 & & & \\ & & \ddots & \ddots & \ddots & & \\ & & & \omega_1 & -(\omega_0+\omega_1) & \omega_0 & \\ & & & & \omega_1 & -\omega_1 \end{bmatrix} \tag{8}$$

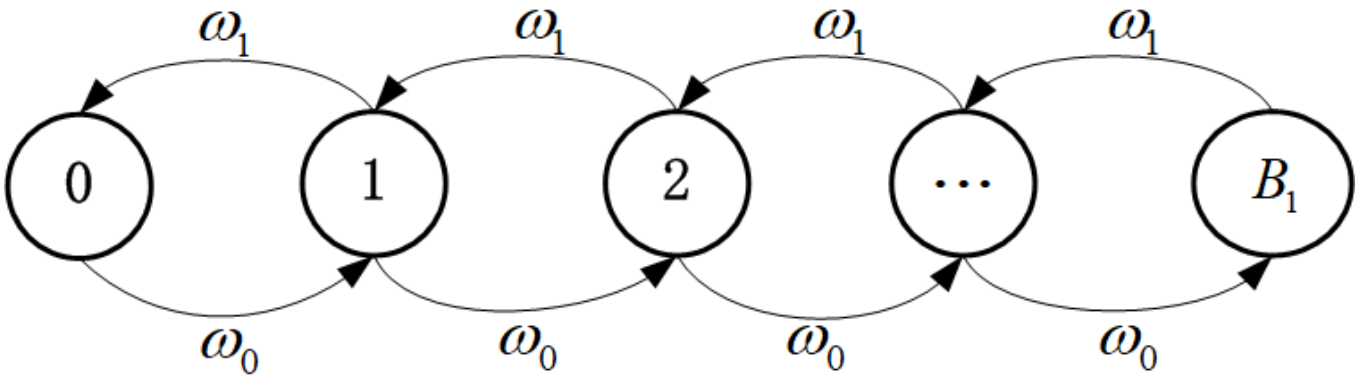

Figure 9. State-transition diagram of the buffer B_1.

The death rate of the first service station (namely, ω_1) is exactly the birth rate of the second service one. $E_2 = \{(b_N(t), b_{N\text{-}1}(t), \ldots, b_i(t), \ldots, b_1(t)), i = 1, \ldots, N, b_i(t) = 0, 1, \ldots, B_i\}$, $b_2(t) = 0, 1, 2, \ldots, B_2$, $b_1(t) = 0, 1, 2, \ldots, B_1$; the state-transition process of both buffer B_1 and B_2 is shown in Figure 10.

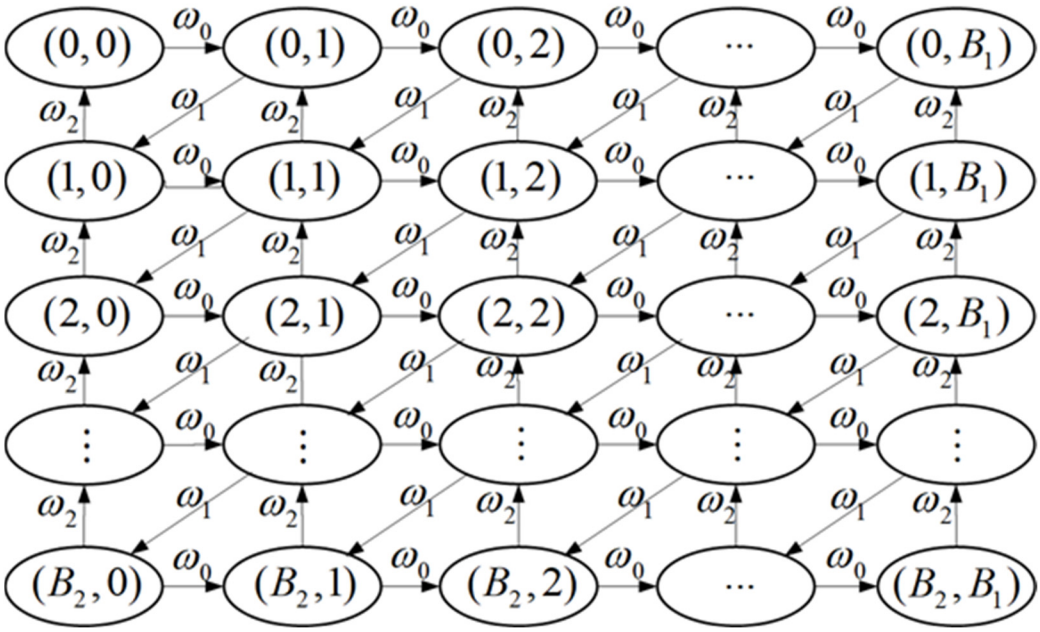

Figure 10. State-transition diagram of the buffer B_1 and B_2.

Considering the Markov property in Figure 10, the state process of nodes is only related to their adjacent nodes' states. Thereby, we can deduce the state-transition matrix Q_2 of E_2 based on Q_1. Firstly, the state transition density matrix of the process $(0, b_1(t)) \rightarrow (0, b_1(t + \Delta t))$, which matches with the first row in Figure 10, can be indicated as Q_1^a in the following context.

$$Q_1^a = \begin{bmatrix} -\omega_0 & \omega_0 & & & & & \\ & -(\omega_0+\omega_1) & \omega_0 & & & & \\ & & -(\omega_0+\omega_1) & \omega_0 & & & \\ & & \ddots & \ddots & \ddots & & \\ & & & & -(\omega_0+\omega_1) & \omega_0 & \\ & & & & & -\omega_1 & \end{bmatrix} \quad (9)$$

The transition rate of state $(r, b_1(t)) \rightarrow (r + 1, b_1(t + \Delta t))$ is exactly the death rate ω_1 of the first station, which means a work-piece is transferred to Queue 2 from Queue 1 ($r = 0, 1,$

$\ldots, B_2 - 1$). The state transition density matrix of such a process, which is indicated as Q_1^b, is shown as Equation (10).

$$Q_1^b = Q_1 - Q_1^a = \begin{bmatrix} 0 & & & & & \\ \omega_1 & 0 & & & & \\ & \omega_1 & 0 & & & \\ & & \ddots & \ddots & & \\ & & & \omega_1 & 0 & \\ & & & & \omega_1 & 0 \end{bmatrix} \tag{10}$$

Accordingly, the transition density matrix of the process $(r + 1, b_1(t)) \to (r, b_1(t + \Delta t))$ is indicated as $\omega_2 I$, which means a part is finished at Queue 2 ($r = 0, 1, \ldots, B_2 - 1$). Additionally, the transition density matrix of $(r, b_1(t)) \to (r, b_1(t + \Delta t))$ is $Q_1^a - \omega_2 I$, wherein $2 \le r \le B_2 - 1$.

As for $(B_2, b_1(t)) \to (B_2, b_1(t + \Delta t))$, the transition density matrix, which matches with the last row in Figure 10, can be shown as the following transformation:

$$(Q_1^a + Q_1^b D_1) - \omega_2 I = \begin{bmatrix} -\omega_0 - \omega_2 & \omega_0 & & & & \\ & -\omega_0 - \omega_2 & \omega_0 & & & \\ & & \ddots & \ddots & & \\ & & & -\omega_0 - \omega_2 & \omega_0 & \\ & & & & & -\omega_2 \end{bmatrix} \tag{11}$$

where $D_1 = \begin{bmatrix} 0 & I & & & \\ & 0 & I & & \\ & & \ddots & \ddots & \\ & & & 0 & I \\ & & & & 0 \end{bmatrix}$.

Hence, Q_2 can be obtained based on Q_1 as the following equation:

$$Q_2 = \begin{bmatrix} Q_1^a & Q_1^b & & & & & \\ \omega_2 I & Q_1^a - \omega_2 I & Q_1^b & & & & \\ & \omega_2 I & Q_1^a - \omega_2 I & Q_1^b & & & \\ & & \ddots & \ddots & \ddots & & \\ & & & \omega_2 I & Q_1^a - \omega_2 I & Q_1^b & \\ & & & & \omega_2 I & Q_1^a + Q_1^b D_1 - \omega_2 I \end{bmatrix} \tag{12}$$

Accordingly, the state process of E_i is a quasi-birth and death process (QBD). The birth rate of the ith queue is the death rate of the $(i - 1)$th queue ($i > 1$). The transition matrix of such a process is Q_{i-1}^b ($i > 1$). The transition matrix of state space $\{(r + 1, h), h \in E_{i-1}, r = 0, 1, \ldots, B_i - 1\}$ to $\{(r, h), h \in E_{i-1}, r = 0, 1, \ldots, B_i - 1\}$ is $\omega_i I$, which means a part is finished by the ith queue. Accordingly, the state-transition matrix Q_i with a higher dimension can also be derived by Q_{i-1} according to the recurrence relation.

$$Q_i = \begin{bmatrix} Q_{i-1}^a & Q_{i-1}^b & & & & & \\ \omega_i I & Q_{i-1}^a - \omega_i I & Q_{i-1}^b & & & & \\ & \omega_i I & Q_{i-1}^a - \omega_i I & Q_{i-1}^b & & & \\ & & \ddots & \ddots & \ddots & & \\ & & & \omega_i I & Q_{i-1}^a - \omega_i I & Q_{i-1}^b & \\ & & & & \omega_i I & Q_{i-1}^a + Q_{i-1}^b D_{i-1} - \omega_i I \end{bmatrix} \tag{13}$$

$2 \le i \le N$.

wherein,

$$Q_i^a = \begin{bmatrix} Q_{i-1}^a & Q_{i-1}^b & & & & & \\ & Q_{i-1}^a - \omega_i I & Q_{i-1}^b & & & & \\ & & Q_{i-1}^a - \omega_i I & Q_{i-1}^b & & & \\ & & & \ddots & \ddots & & \\ & & & & Q_{i-1}^a - \omega_i I & Q_{i-1}^b & \\ & & & & & Q_{i-1}^a + Q_{i-1}^b D_{i-1} - \omega_i I \end{bmatrix},$$

$$D_{i-1} = \begin{bmatrix} 0 & I & & & \\ & 0 & I & & \\ & & \ddots & \ddots & \\ & & & 0 & I \\ & & & & 0 \end{bmatrix}, \; Q_i^b = Q_i - Q_i^a.$$

5.2. State Space Equations

The exact performance of small-scale systems can be computed, avoiding the large-scale matrix Q_N. Suppose $\mathbf{Y} = (\mathbf{Y_0}, \mathbf{Y_1}, \mathbf{Y_2}, \ldots, \mathbf{Y_N})$ is the steady-state solution of the stochastic service system model. The following equation should be satisfied according to the equilibrium condition.

$$\mathbf{Y}Q_N = 0 \tag{14}$$

where Q_N is computed in terms of Equation (13). Thus, the following equations can be obtained.

$$\mathbf{Y_0}Q_{N-1}^a + \mathbf{Y_1}(\omega_N I) = \mathbf{0} \tag{15}$$

$$\mathbf{Y_0}Q_{N-1}^b + \mathbf{Y_1}(Q_{N-1}^a - \omega_N I) + \mathbf{Y_2}(\omega_N I) = 0 \tag{16}$$

$$\mathbf{Y_{i-1}}Q_{N-1}^b + \mathbf{Y_i}(Q_{N-1}^a - \omega_N I) + \mathbf{Y_{i+1}}(\omega_N I) = 0 \tag{17}$$

$$\mathbf{Y_{N-1}}Q_{N-1}^b + \mathbf{Y_N}(Q_{N-1}^a + Q_{N-1}^b D_{N-1} - \omega_N I) = 0 \tag{18}$$

The following constraint is given by

$$\mathbf{Y_0}e_0 + \sum_{i=1}^{N} \mathbf{Y_i}e_1 = 1 \tag{19}$$

where the dimension of all 1 column vectors e_0 and e_1 is the same as Y_0 and Y_1.

Let $C = (-\omega_N I)^{-1}$, $\mathbf{Y_{i+1}}$ can be obtained according to Equation (17).

$$\mathbf{Y_{i+1}} = \mathbf{Y_{i-1}}Q_{N-1}^b C + \mathbf{Y_i}[Q_{N-1}^a - \omega_N I]C \tag{20}$$

$$\mathbf{Y}_2 = \mathbf{Y_0}Q_{N-1}^b C + \mathbf{Y_1}[Q_{N-1}^a - \omega_N I]C \tag{21}$$

$$\mathbf{Y}_1 = \mathbf{Y_0}Q_{N-1}^a C \tag{22}$$

In order to simplify the derivative process, we give the following substitution parameters:

$$H_1 = 0, \;\; H_2 = Q_{N-1}^b C, \;\; G_1 = I, \;\; G_2 = [Q_{N-1}^a - \omega_N I]C \tag{23}$$

$$H_{i+1} = H_{i-1}Q_{N-1}^b C + H_i[Q_{N-1}^a - \omega_N I]C, \qquad 1 < i < B_N - 1 \tag{24}$$

$$G_{i+1} = G_{i-1}Q_{N-1}^b C + G_i[Q_{N-1}^a - \omega_N I]C, \qquad 1 < i < B_N - 1 \tag{25}$$

$\mathbf{Y_2}$ can be represented as ($\mathbf{Y_0}H_2$ + $\mathbf{Y_1}G_2$) according to Equations (21) and (23). Then, $\mathbf{Y_i}$ can also be expressed by $\mathbf{Y_0}$ and $\mathbf{Y_1}$ through iterative computing.

$$\mathbf{Y_i} = \mathbf{Y_0}H_i + \mathbf{Y_1}G_i, \qquad 1 \le i \le B_N - 1 \tag{26}$$

$\mathbf{Y_i}$ can be further expressed containing only $\mathbf{Y_0}$ using Equation (22).

$$\mathbf{Y_i} = \mathbf{Y_0}(H_i + Q_{N-1}^a C G_i), \qquad 1 \le i \le B_N - 1 \tag{27}$$

We further calculate $\mathbf{Y_N}$ by Equation (18).

$$\begin{aligned}\mathbf{Y_N} &= -\mathbf{Y_{N-1}} Q_{N-1}^{b} (Q_{N-1}^{a} + Q_{N-1}^{b} D_{N-1} - \omega_N I)^{-1} \\ &= -\mathbf{Y_0} (H_{N-1} + Q_{N-1}^{a} C G_{N-1}) Q_{N-1}^{b} (Q_{N-1}^{a} + Q_{N-1}^{b} D_{N-1} - \omega_N I)^{-1}\end{aligned} \tag{28}$$

In order to simplify the derivative process, we further give the following substitution variable:

$$R_i = H_i + Q_{N-1}^{a} C G_i, \quad 1 \le i \le B_N - 1, \quad R_N = -R_{N-1} Q_{N-1}^{b} (Q_{N-1}^{a} + Q_{N-1}^{b} D_{N-1} - \omega_N I)^{-1} \tag{29}$$

Thus, $\mathbf{Y_i} = \mathbf{Y_0} R_i$, $I = 1, 2, \ldots, N$. By adding together Equations (15) and (18), we can obtain the following formula containing only $\mathbf{Y_0}$:

$$\mathbf{Y}_0 [Q_{N-1} + \sum_{i=1}^{N-1} R_i Q_{N-1} + R_N (Q_{N-1}^{a} + Q_{N-1}^{b} D_{N-1})] = 0 \tag{30}$$

Equation (19) can also be shown as follows:

$$\mathbf{Y}_0 (e_0 + \sum_{i=1}^{N} R_i e_1) = 1 \tag{31}$$

In conclusion, $\mathbf{Y_0}$ can be determined by the following linear inhomogeneous equations:

$$\begin{bmatrix} [Q_{N-1} + \sum\limits_{i=1}^{N-1} R_i Q_{N-1} + R_N (Q_{N-1}^{a} + Q_{N-1}^{b} D_{N-1})]^{T} \\ (e_0 + \sum\limits_{i=1}^{N} R_i e_1)^{T} \end{bmatrix} \mathbf{Y}_0{}^{T} = \begin{bmatrix} 0_{M_{N-1} \times 1} \\ 1 \end{bmatrix} \tag{32}$$

wherein, $M_{N-1} = \prod_{i=1}^{N-1} (B_i + 1)$. Additionally, $\mathbf{Y}$ can be further calculated by Equations (27) and (28).

5.3. Vulnerability Quantification

The disruptive event $E(m_i, t_e, d_e)$ will bring different levels of impact on system production performance, which has distinct temporal and spatial attributes owing to the disruption location and duration. According to Equations (1) and (3), the transient vulnerability of $E(m_i, t_e, d_e)$ is determined by the WIPs and vacancies condition at the moment of t_e.

From the foregoing definition, both terminal vulnerability and bottleneck vulnerability are required to be quantified. In Equation (1), according to little's law, Transient TTD in t_e is computed based on work-pieces of downstream buffers and stations after m_i.

$$TD_i(t_e) = \frac{\sum_{h=i+1}^{N} L_h(t_e)}{(1 - ST_N)\omega_N} = \frac{\sum_{h=i+1}^{N} [b_h(t_e) + x_{m_h}(t_e)]}{(1 - ST_N)\omega_N} \tag{33}$$

where $L_h(t_e)$ is the queue length of the hth service station, $b_h(t_e)$ is the number of WIPs in the hth buffer, and $x_{m_h}(t_e)$ is the variate that indicates whether there is a work-piece in m_h, which equals to 1 if there is one, 0 otherwise. Note that both $b_h(t_e)$ and $x_{m_h}(t_e)$ should be given as the input condition. The probability of the starvation of the last station is ST_N, which is calculated by

$$ST_N = P\{L_N = 0\} = \sum_{\xi \in E_{NS}} Y_\xi \tag{34}$$

where L_N is the queue length of the last station, Y_ξ is the probability of state ξ, and state space E_{NS} is shown as:

$$E_{NS} = \{0, b_{N-1}(t), \ldots, b_i(t), \ldots, b_1(t), i = 1, \ldots, N-1, b_i(t) = 0, 1, \ldots, B_i\} \tag{35}$$

Transient TTW for the repair process of m_i, namely the opportunity window that the first work-piece after repair catches up with the foregoing last work-piece exactly at m_N, can be quantified by the following equation.

$$TW_i(t_e) = \frac{\sum_{h=i+1}^{N} L_h(t_e)}{(1 - ST_N)\omega_N} - \sum_{h=i}^{N-1} \frac{1}{\omega_h} = \frac{\sum_{h=i+1}^{N} [b_h(t_e) + x_{m_h}(t_e)]}{(1 - ST_N)\omega_N} - \sum_{h=i}^{N-1} \frac{1}{\omega_h} \tag{36}$$

The steady TTD of a disruptive event $E(m_i, t_e, d_e)$ can be computed by the average queue length between m_i and m_N, which is shown as:

$$\overline{TD_i} = \frac{EL_i^{TTD}}{(1 - ST_N)\omega_N} \tag{37}$$

EL_i^{TTD} represents the expected queue length between m_i and m_N in the steady state. In the above equation, the steady joint probability distribution of each queue length can be indicated as the following equation:

$$P\{\bigcap_{h=1}^{N}(L_h = l_h)\} = \sum_{\xi \in E_N} Y_\xi, E_N = \{(b_N, b_{N-1}, \ldots, b_i, \ldots, b_1), b_i = 1, \ldots, B_i\} \tag{38}$$

EL_i^{TTD} can be determined by the following equation:

$$EL_i^{TTD} = \sum_{\xi \in E_N} [Y_\xi \sum_{h=i+1}^{N} b_h(\xi)] \tag{39}$$

where $b_h(\xi)$ is the number of work pieces in Queue h under the state ξ.

The steady TTW can also be computed by the average queue length.

$$\overline{TW_i} = \frac{EL_i^{TTD}}{(1 - ST_N)\omega_N} - \sum_{h=i}^{N-1} \frac{1}{\omega_h} \tag{40}$$

As for the bottleneck-dominated vulnerability, the BTD of $E(m_i, t_e, d_e)$ is determined by the WIPs and vacancies condition at the moment of t_e. Suppose a disruptive event occurs in m_i, and the bottleneck station is m_k. If $i \leq k$, BTD is the time interval for all WIPs in line L_2 passing through m_k. If $i > k$, BTD is the time interval for all buffers in line L_2 becoming full.

Therefore, if $I > k$, the transient BTD of $E(m_i, t_e, d_e)$ can be computed by the sojourn time of the last WIP before disruption event between m_i and m_k. If $i > k$, the transient BTD of $E(m_i, t_e, d_e)$ can be computed by the time that all vacancies between m_i and m_k become full.

$$BD_i(t_e) = \begin{cases} \frac{\sum_{h=i+1}^{k} L_h(t_e)}{SB_k \omega_k}, & i < k \\ 0, & i = k \\ \frac{\sum_{h=k+1}^{i} [B_h - L_h(t_e)]}{SB_k \omega_k}, & i > k \end{cases} \tag{41}$$

where SB_k is the probability that m_k is neither starved nor blocked. SB_k is calculated by the following equation:

$$SB_k = \sum_{\xi \in E_{BS-k}} Y_\xi, \quad E_{BS-k} = \{b_N, b_{N-1}, \ldots, b_{k+1} \neq B_{k+1}, b_k \neq 0, \ldots, b_1\}, b_k = 0, 1, \ldots, B_k \tag{42}$$

Bottleneck station m_k is determined by the starvation and blocking probability.

$$\begin{array}{l} S_h = |ST_{h+1} - BL_h| + |ST_h - BL_{h-1}|, \quad h = 1, 2, \ldots, N-1 \\ S_0 = |ST_1 - BL_0|, \quad S_N = |ST_N - BL_{N-1}| \end{array} \tag{43}$$

where the starvation probability of m_h is obtained by

$$ST_h = \sum_{\xi \in E_{ST-h}} Y_\xi, \quad E_{ST-h} = \{b_N, b_{N-1}, \ldots, b_h = 0, \ldots, b_1\}, b_h = 0, 1, \ldots, B_h \tag{44}$$

and the blocking probability of m_h is obtained by

$$BL_h = \sum_{\xi \in E_{BL-h}} Y_\xi, \quad E_{BL-h} = \{b_{N-1}, \ldots, b_h, b_{h+1} = B_{h+1}, \ldots, b_1\}, b_h = 0, 1, \ldots, B_h \tag{45}$$

Queue length at m_h is obtained by

$$L_h(t_e) = [b_h(t_e) + x_{m_h}(t_e)] \tag{46}$$

Steady BTD can be computed by the average queue length.

$$\overline{BD_i} = \begin{cases} \frac{EL_{i-k}^{BTD}}{SB_k\omega_k}, & i < k \\ 0, & i = k \\ \frac{\sum_{h=k+1}^{i} B_h - EL_{i-k}^{BTD}}{SB_k\omega_k}, & i > k \end{cases} \tag{47}$$

EL_{i-k}^{BTD} represents the expected queue length between m_i and m_k, which can be computed in a similar way.

$$EL_{i-k}^{BTD} = \begin{cases} \sum\limits_{\xi \in E_{BS-k}} [Y_\xi \sum_{h=i+1}^{k} b_h(\xi)], & i < k \\ 0, & i = k \\ \sum\limits_{\xi \in E_{BS-k}} [Y_\xi \sum_{h=k+1}^{i} b_h(\xi)], & i > k \end{cases} \tag{48}$$

Accordingly, transient BTW for the repair process of m_i, namely the opportunity window that the first work-piece after repair catches up with the foregoing last work-piece exactly at the bottleneck station m_k, can be quantified by the following equation:

$$BW_i(t_e) = \begin{cases} \frac{\sum_{h=i+1}^{k} L_h(t_e)}{SB_k\omega_k} - \sum_{h=i}^{k-1} \frac{1}{\omega_h}, & i < k \\ 0, & i = k \\ \frac{\sum_{h=k+1}^{i} [B_h - L_h(t_e)]}{SB_k\omega_k} - \sum_{h=k}^{i-1} \frac{1}{\omega_h}, & i > k \end{cases} \tag{49}$$

The steady BTW can also be computed by the average queue length.

$$\overline{BW_i} = \begin{cases} \frac{EL_{i-k}^{BTD}}{SB_k\omega_k} - \sum_{h=i}^{k-1} \frac{1}{\omega_h}, & i < k \\ 0, & i = k \\ \frac{\sum_{h=k+1}^{i} B_h - EL_{i-k}^{BTD}}{SB_k\omega_k} - \sum_{h=k}^{i-1} \frac{1}{\omega_h}, & i > k \end{cases} \tag{50}$$

Therefore, the transient vulnerability effect on the terminal station can be quantified for each disturbance event $E(m_i, t_e, d_e)$ as follows:

$$V_i^T(t_e) = \begin{cases} 0, & d_e \le TW_i(t_e) \\ \lambda_i\omega_N(1 - ST_N)[d_e - TW_i(t_e)], & d_e > TW_i(t_e) \end{cases} \tag{51}$$

The steady vulnerability effect of m_i on the final station can be quantified by

$$V_i^T = \begin{cases} 0, & d_e \le \overline{TW_i} \\ \lambda_i\omega_N(1 - ST_N)(d_e - \overline{TW_i}), & d_e > \overline{TW_i} \end{cases} \tag{52}$$

The transient vulnerability effect on the system bottleneck can be quantified for each disturbance event $E(m_i, t_e, d_e)$ as follows:

$$V_i^B(t_e) = \begin{cases} 0, & d_e \le BW_i(t_e) \\ \lambda_i\omega_k[d_e - BW_i(t_e)], & d_e > BW_i(t_e) \end{cases} \tag{53}$$

The steady vulnerability effect of m_i on the system output can be quantified by

$$V_i^B = \begin{cases} 0, & d_e \le \overline{BW_i} \\ \lambda_i\omega_k(d_e - \overline{BW_i}), & d_e > \overline{BW_i} \end{cases} \tag{54}$$

6. Case Study

The rapid replacement of mobile phone products poses a serious challenge to its assembly system. Frequent product replacement results in frequent switching of the configuration structure of the production line, which leads to the instability of the production process and the loss of production capacity. The mobile phone assembly process is very complicated and has many procedures, including dozens of procedures such as mainboard inspection, camera welding, antenna bracket installation, camera fixing, and button board welding. Due to factors such as frequent product replacement, equipment failure, and adjustment of line change parameters, the production capacity of the production line is often lost. At present, most mobile phone assembly companies belong to

foundries, with meager profits. The loss of capacity due to frequent interruptions will seriously affect corporate profits. Therefore, in order to ensure the stable production capacity of the production line under high-frequency disturbance, it is very important to carry out vulnerability analysis and control strategies.

The Digital Twin System (DTS) is a 3D design and simulation optimization system designed by our team for the characteristics and needs of the 3C manufacturing industry. It has strong 3D near-physical simulation capabilities and good scalability. Figure 11 is the virtual simulation platform and physical production line of the mobile phone assembly line built by DTS, respectively. The entire project is based on digital twin technology, which not only supports open architecture design, rapid reconfiguration of production lines, distributed integration testing, transparent monitoring, high-fidelity hardware-in-the-loop simulation, rapid custom design of the entire line, and other application modalities, but also includes a fully automatic production line, custom design platform, intelligent control system, and other parts.

(**a**) (**b**)

Figure 11. Mobile phone assembly line. (**a**) Virtual Simulation Platform. (**b**) Physical assembly line.

DTS is mainly composed of four functional modules including basic management, near-physical simulation, multi-view synchronization, performance analysis, and regulation, and each module contains multiple sub-functions. The main function modules and main interface of the system are shown in Figure 12 respectively. Figure 12a is the main interface of the digital twin system, which mainly includes functional areas such as the 3D view window, function menu area, component library, model BOM tree, and model attribute management. Figure 12b is the scene layout of the system interface, which can design the layout of the production line in the 3D scene. Figure 12c is the model property management interface, which can set the near-physical properties of the 3D model. Figure 12d is the scripting interface, which can Script control of equipment actions and WIP flow in the production line. Figure 12e is the PLC connection management interface, which can establish a communication channel between physical equipment and virtual models. Figure 12f is the performance analysis and control interface, which can analyze the performance of the production line and iteratively optimize the design of the production line. The vulnerability analysis method proposed in this paper is an important theoretical basis for the performance analysis and control module. Based on this method, the module can realize the real-time analysis of the production line performance. Simulate disturbance events, quantify vulnerability indicators, and then formulate appropriate disturbance control strategies to avoid production residual losses.

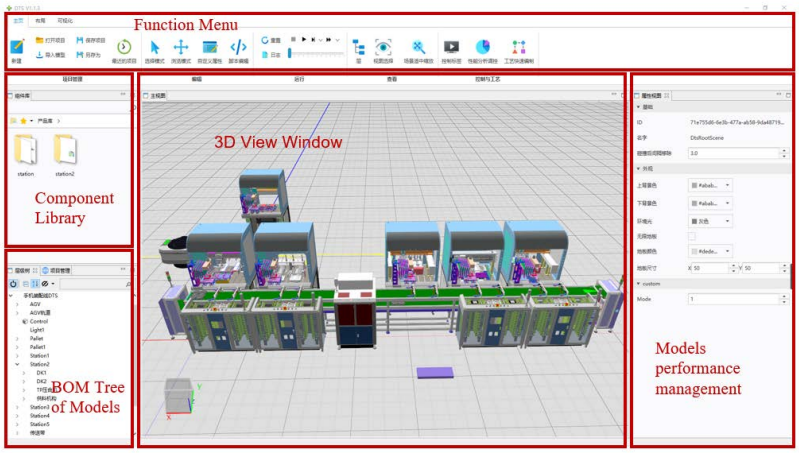

(**a**)

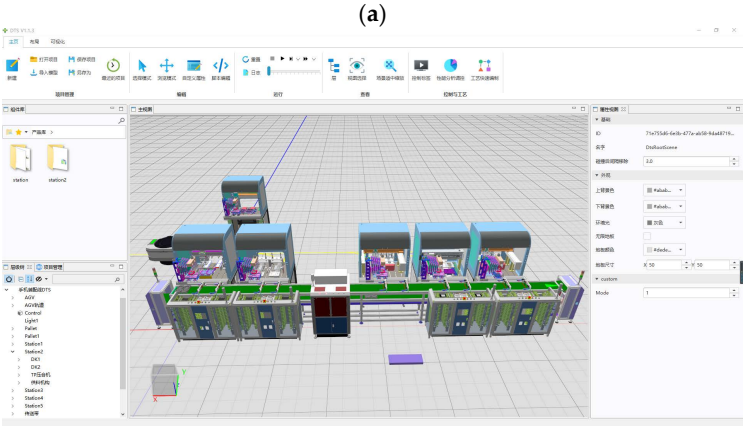

(**b**)

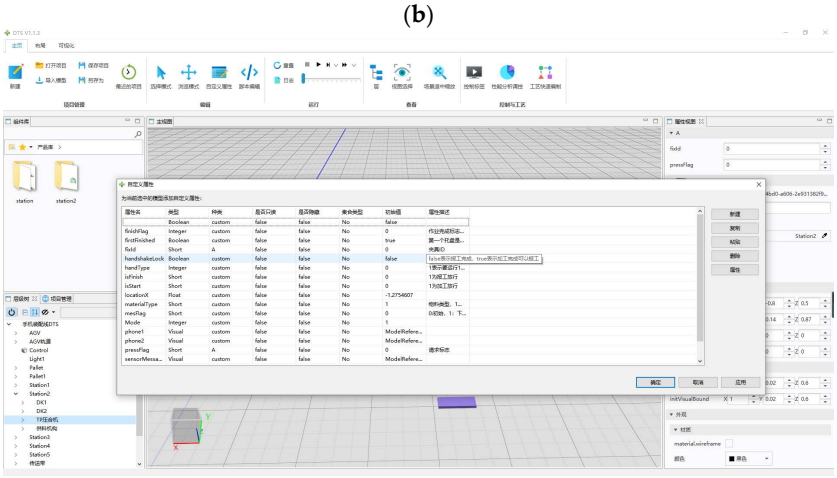

(**c**)

Figure 12. *Cont*.

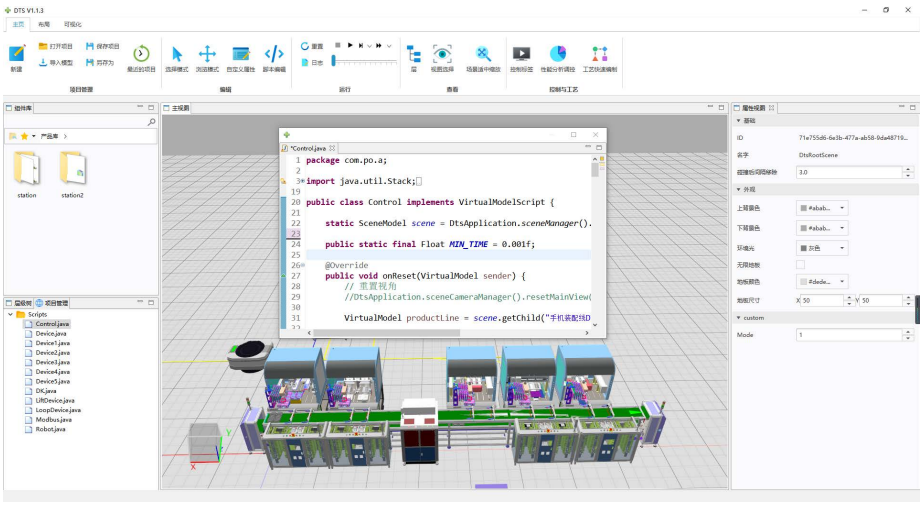

(**d**)

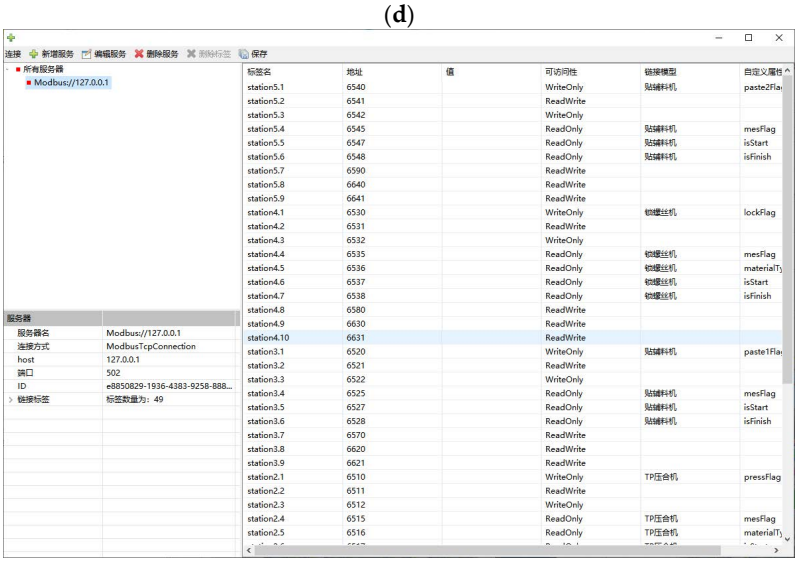

(**e**)

(**f**)

Figure 12. Introduction to the main function interface of DTS. (**a**) Digital twin interface. (**b**) Scene layout management interface. (**c**) Models' property management interface. (**d**) Script writing interface. (**e**) PLC connection management interface. (**f**) Performance analysis and control interface.

Combining the theoretical research results in this paper, this chapter develops a vulnerability analysis application that supports disturbance simulation, vulnerability quantification, and disturbance control. Additionally, it encapsulate it as a functional component into the performance and analysis control module of the digital twin system, as shown in Figure 13. In the vulnerability quantitative analysis and control strategy module, after inputting fault data, the "Vulnerability Index Solving" function can quantify the vulnerability index of the production line, generate a production line performance analysis chart, and display the quantification results. The "disturbance control strategy" function can generate the control strategy when the equipment fails.

Figure 13. Vulnerability quantitative analysis and disturbance control strategies interface.

The analytical models described in the previous sections can accurately evaluate the performance of production systems under dynamic disruptions, and the case studies in this section aim to validate the vulnerability quantification method. Select some of the processes in the mobile phone assembly process for virtual simulation, namely sticking double-sided tape, dispensing, TP pressing, back cover locking screws, pasting accessories, etc. Suppose the production line consists of 8 tandem queues, namely 8 stations and 7 buffers. The configuration parameters of the line are listed in Table 1. It is supposed that the first station is never starved.

Table 1. Configuration information and reliability parameters.

	Queue 1	**Queue 2**	**Queue 3**	**Queue 4**	**Queue 5**	**Queue 6**	**Queue 7**	**Queue 8**
Buffer capacity	/	2	2	2	2	2	2	2
Service rate μ_i	4.5	4.3	4.1	4.3	4.5	4.2	4.5	4.5
Failure rate λ_i	0.036	0.040	0.031	0.029	0.029	0.040	0.034	0.034

Note that transient vulnerability is determined by the monitoring buffer/machine occupancy dynamics. Transient vulnerability evaluation is helpful for real-time decision support such as opportunity maintenance. It can be inferred by real-time queue lengths using Equations (33), (36), (41), and (49). On account of the number of work-pieces in buffers being variable, a steady evaluation is more valuable for configuration design or vulnerability control.

Figure 14 exhibits the steady vulnerability evaluation results. Steady TTD, TTW, BTD, and BTW results are used to illustrate the temporal and spatial attributes. As shown in Figure 14, $\overline{BD_2}$ and $\overline{BW_2}$ equal 0. Thus, M_1 (Queue 2) can be inferred as the main bottleneck machine according to Equations (47) and (50). In terms of the evaluation of terminal vulnerability, both TTD and TTW gradually diminish with the decrease in distance from the terminal machine. From the perspective of bottleneck vulnerability, both the BTD and BTW gradually increase as the distance is augmented from the bottleneck machine. Despite the obvious trend of vulnerability, this paper presents a quantitative approach that is the basis of further precise performance control strategies. Note that it will lead to large errors if the TTD and BTD are considered as the TTW and BTW in responsive controlling decisions. For example, in order not to cause any system production loss, the permitted opportunity maintenance window for machines should be determined by the BTW instead of the BTD.

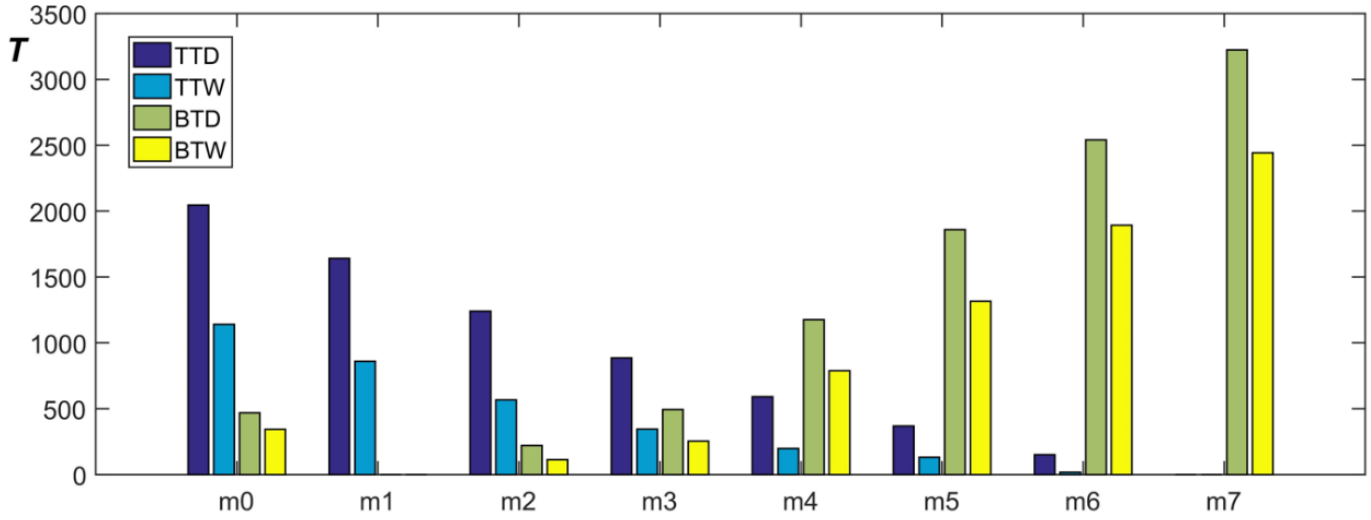

Figure 14. Steady TTD, TTW, BTD, and BTW results.

The vulnerability delay effect can be clearly displayed in Figures 15 and 16. An obvious time delay of disruption can be evaluated via the proposed approach. After certain critical time points, namely steady TTWs in Figure 15 and steady BTWs in Figure 16, the vulnerability effect will be linearly related to the repair time d_e with different slopes. The vulnerability effects of the bottleneck machine (namely M_1) are obvious. However, the terminal vulnerability of M_0 will surpass M_1 at a certain d_e, becoming the most vulnerable machine. On the whole, the bottleneck vulnerability effect turns out to be more obvious when it is farther away from M_1. Accordingly, failure fluctuations of the terminal machine can be well assessed via the results of terminal vulnerability in Figure 15. Further controlling decisions (for example, permitted opportunity maintenance intervals) are available to avoid the stockout of the downstream supply chain. Additionally, failure fluctuations of the whole system output can be well assessed via the results of bottleneck vulnerability in Figure 16. Additional controlling decisions (for example, buffer reallocation, line rebalancing, or permitted opportunity maintenance window for individual equipment) turn out to be available to keep normal production output.

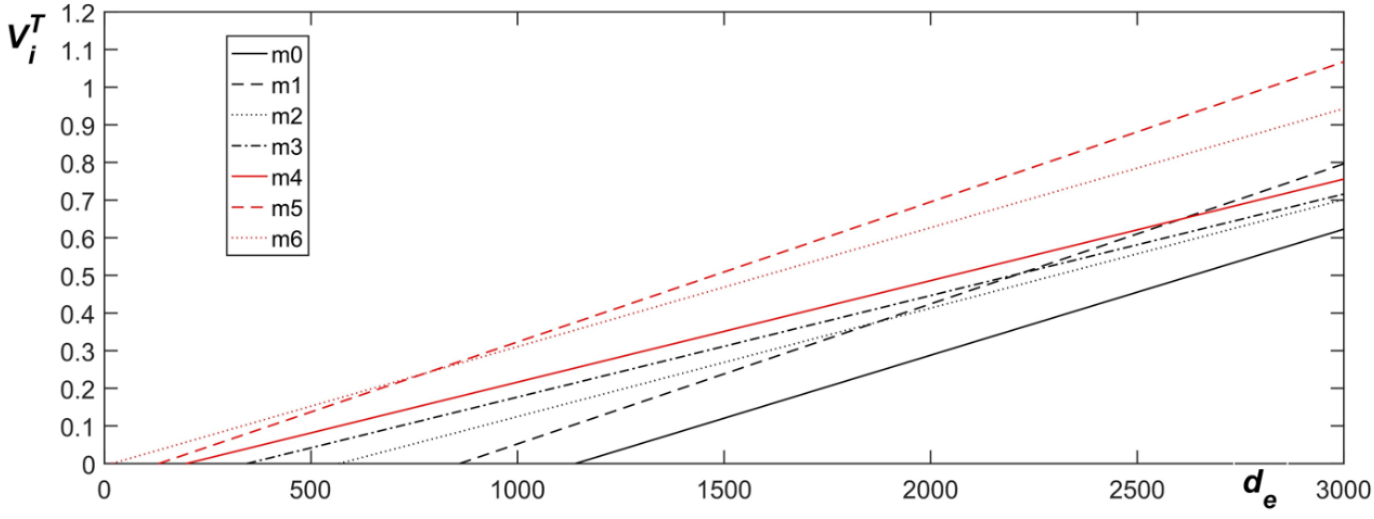

Figure 15. Terminal vulnerability delay and its evolutional curve.

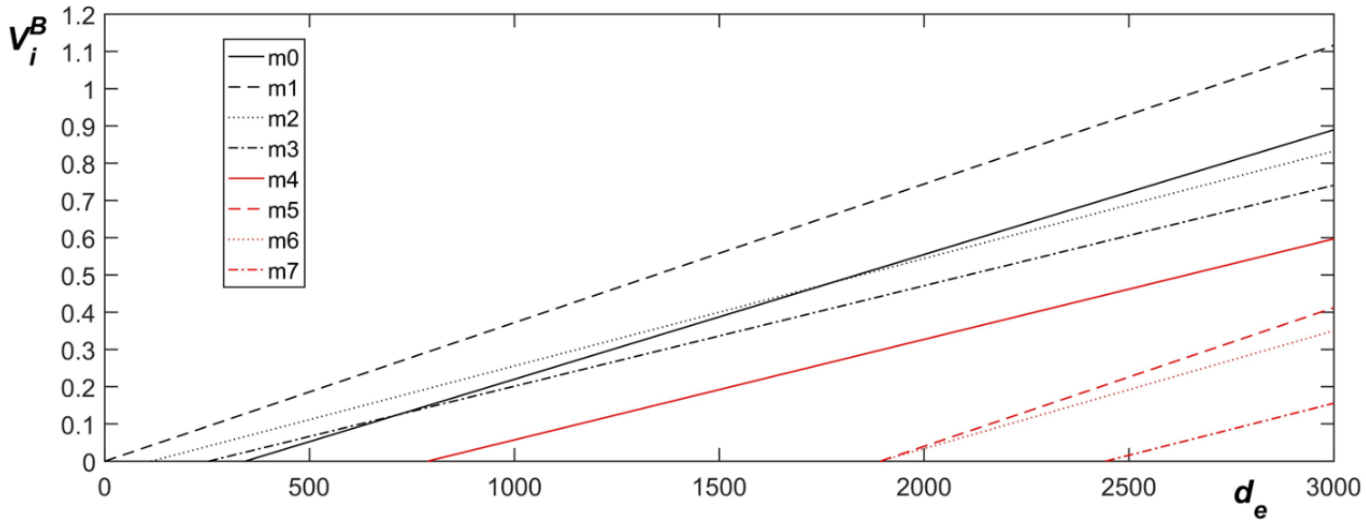

Figure 16. Bottleneck vulnerability delay and its evolutional curve.

Apart from the distinct temporal and spatial characteristics when determining the null points, the evolutional curve of vulnerability is closely sensitive to the failure rate of m_i and the service rate of the line. As shown in Figure 15 and Equation (52), terminal vulnerability is quite sensitive to failure rate λ_i and the average processing speed of the last queue, while bottleneck vulnerability is determined by the average processing speed of the bottleneck.

This paper affords an analytical model of vulnerability evaluation under sudden disruptive events. The computing speed of the analytical model is faster than the normal event simulation model. The proposed vulnerability evaluation model is the basis (mainly the four performance indicators) for further quick decisions (such as reconfiguration optimization) under disruptions in the digital twin system. The four performance indicators are steady results. To verify them, we use Plant Simulation software to build the simulation model shown in the Figure 17, and conduct simulation experiments.

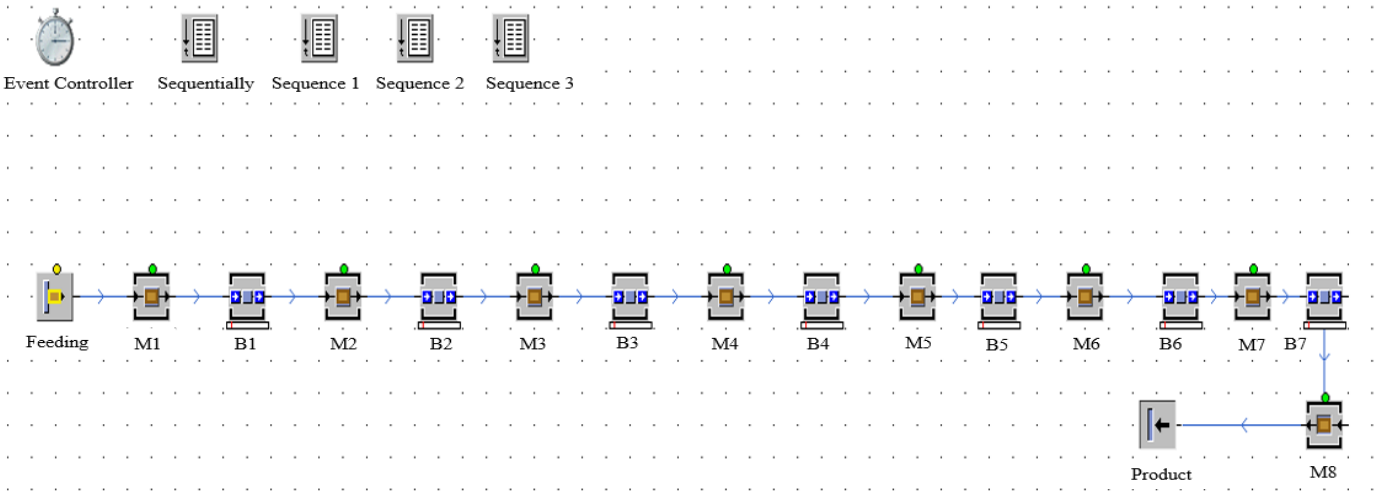

Figure 17. Simulation model of a mobile phone assembly line.

Table 2 shows the numerical comparison of the analytical model and the simulation model of the terminal time delay. The comparison result shows that the analytical results of Figure 15 are basically anastomotic with the real assembly scenario, and the evaluating errors lie in 2% for all machines.

Table 2. Terminal time delay quantization results.

Machine	Analytical Method	Simulation Method	Evaluate Errors
m0	1202.75	1198.45	0.35%
m1	891.63	897.11	0.61%
m2	595.97	588.29	1.2%
m3	385.98	382.29	0.95%
m4	224.53	222.86	0.74%
m5	152.85	151.49	0.89%
m6	42.16	42.47	0.73%

7. Conclusions

This paper explores the nature of dynamics analysis of production systems and proposes a vulnerability evaluation approach for mobile phone assembly lines under a resilient system analytic frame. The vulnerability effect on the terminal and bottleneck machine is surveyed based on the stochastic production system model, wherein temporal and spatial attributes are expounded via vulnerability delay phenomena. Four special vulnerability indicators, namely TTD, TTW, TTD, and TTW, are defined. Afterward, the transition matrix of the production system ($N + 1$ machines and N buffers) is obtained by a recursive derivation means. Transient and steady vulnerabilities are evaluated in two different modes, terminal vulnerability and bottleneck vulnerability, respectively. The theoretical research is then translated into practical tools. An application program for brittleness analysis and evaluation is developed and applied to the digital twin system independently developed by the team to solve practical problems.

Potential future work can be divided into two aspects, vulnerability evaluation and vulnerability control, respectively. On the one hand, the proposed exact evaluating approach is valuable for the future approximative model of large production systems. Additionally, different failure distributions such as the phase-type distribution should be studied. On the other hand, based on the proposed vulnerability analysis approach, vulnerability control through reconfiguration planning or preventive maintenance is the prospective research issue.

Author Contributions: Conceptualization, D.Z.; formal analysis, D.Z., Y.P. and Q.L.; investigation, D.Z., Y.P. and Q.L.; methodology, D.Z.; writing—original draft preparation, D.Z.; writing—review and editing, Y.P. All authors have read and agreed to the published version of the manuscript.

Funding: This project is supported by the National Key R & D Program of China (2019YFB170620X), National Natural Science Foundation of China (Grant No. 51805095, 71971181), The Guangdong Provincial Natural Science Foundation (Grant No. 2020A1515010879), Hong Kong Scholar Program (XJ2019058), The Science and Technology Planning Project of Guangdong Province of China (Grant No. 2019B090916002, 2019A050503010).

Institutional Review Board Statement: Not applicable.

Informed Consent Statement: Not applicable.

Data Availability Statement: Not applicable.

Conflicts of Interest: The authors declare no conflict of interest.

Abbreviations

SVA	system vulnerability analysis
TTD	terminal time delay
TTW	terminal time window
BTD	bottleneck time delay
BTW	bottleneck time window
$TD_i(t_e)$	TTD of m_i at time moment t_e
$TW_i(t_e)$	TTW of m_i at time moment t_e
$BD_i(t_e)$	BTD of m_i at time moment t_e
$BW_i(t_e)$	BTW of m_i at time moment t_e
$E(m_i, t_e, d_e)$	disruption event of m_i at t_e, with the duration time d_e
μ_i	servicing rate of m_i without consideration of failures (deterministic distribution)

λ_i	the failure rate of m_i
ω_i	the servicing rate of m_i with consideration of station failure
$L_h(t_e)$	the queue length of the hth station, with the expected queue length L_h
$b_h(t_e)$	the number of work-pieces in the hth buffer, with the expected value b_h
ST_N	the probability of the starvation of the last station
SB_k	the probability that m_k is neither starved or blocked
EL_i^{TTD}	expected queue length between m_i and m_N
EL_{i-k}^{BTD}	expected queue length between m_i and m_k
$V_i^T(t_e)$	transient vulnerability on the terminal station at t_e, with the steady value V_i^T
$V_i^B(t_e)$	transient vulnerability on the system bottleneck, with the steady value V_i^B

References

1. Li, J.; Meerkov, S.M. Summary of Main Facts of Production Systems Engineering. In *Production Systems Engineering*; Springer: Boston, MA, USA, 2009; pp. 1–8.
2. Matsuo, H. Implications of the Tohoku earthquake for Toyota's coordination mechanism: Supply chain disruption of automotive semiconductors. *Int. J. Prod. Econ.* **2015**, *161*, 217–227. [CrossRef]
3. Opritescu, D.; Hartmann, C.; Riedl, W.; Ritter, M.; Volk, W. Low-Risk bypassing of machine failure scenarios in automotive industry press shops by releasing overall capacity of the production networks. *J. Manuf. Syst.* **2019**, *52*, 121–130. [CrossRef]
4. Zhang, W.J.; van Luttervelt, C.A. Toward a resilient manufacturing system. *CIRP Ann. Manuf. Technol.* **2011**, *60*, 469–472. [CrossRef]
5. Barker, K.; Ramirez-Marquez, J.E.; Rocco, C.M. Resilience-based network component importance measures. *Reliab. Eng. Syst. Saf.* **2013**, *117*, 89–97. [CrossRef]
6. Hosseini, S.; Barker, K.; Ramirez-Marquez, J.E. A review of definitions and measures of system resilience. *Reliab. Eng. Syst. Saf.* **2016**, *145*, 47–61. [CrossRef]
7. Henry, D.; Ramirez-Marquez, J.E. Generic metrics and quantitative approaches for system resilience as a function of time. *Reliab. Eng. Syst. Saf.* **2012**, *99*, 114–122. [CrossRef]
8. Xiang, Y.; Mo, R.; Qiao, H. An Evaluation Method for Brittle Source of the Key Procedure in Complex Parts' Manufacturing. *Math. Probl. Eng.* **2018**, *2018*, 1952674. [CrossRef]
9. Gao, G.B.; Yue, W.H.; Ou, W.C.; Tang, H. Vulnerability evaluation method applied to manufacturing systems. *Reliab. Eng. Syst. Saf.* **2018**, *180*, 255–265.
10. Nakatani, J.; Tahara, K.; Nakajima, K.; Daigo, I.; Kurishima, H.; Kudoh, Y.; Moriguchi, Y. A graph theory-based methodology for vulnerability assessment of supply chains using the life cycle inventory database. *Omega-Int. J. Manag. Sci.* **2018**, *75*, 165–181. [CrossRef]
11. Gao, L.; Shen, W.M.; Li, X.Y. New Trends in Intelligent Manufacturing. *Engineering* **2019**, *5*, 619–620. [CrossRef]
12. Tao, F.; Qi, Q.L.; Wang, L.H.; Nee, A.Y.C. Digital Twins and Cyber-Physical Systems toward Smart Manufacturing and Industry 4.0: Correlation and Comparison. *Engineering* **2019**, *5*, 653–661. [CrossRef]
13. Zhang, H.; Liu, Q.; Chen, X.; Zhang, D.; Leng, J.W. A Digital Twin-Based Approach for Designing and Multi-Objective Optimization of Hollow Glass Production Line. *IEEE Access* **2017**, *5*, 26901–26911. [CrossRef]
14. Liu, Q.; Zhang, H.; Leng, J.W.; Chen, X. Digital twin-driven rapid individualised designing of automated flow-shop manufacturing system. *Int. J. Prod. Res.* **2019**, *57*, 3903–3919. [CrossRef]
15. Zhuang, C.B.; Liu, J.H.; Xiong, H. Digital twin-based smart production management and control framework for the complex product assembly shop-floor. *Int. J. Adv. Manuf. Technol.* **2018**, *96*, 1149–1163. [CrossRef]
16. Cai, B.P.; Xie, M.; Liu, Y.H.; Liu, Y.L.; Feng, Q. Availability-based engineering resilience metric and its corresponding evaluation methodology. *Reliab. Eng. Syst. Saf.* **2018**, *172*, 216–224. [CrossRef]
17. Ouyang, M.; Duenas-Osorio, L. Time-dependent resilience assessment and improvement of urban infrastructure systems. *Chaos* **2012**, *22*, 11. [CrossRef]
18. Zio, E. Challenges in the vulnerability and risk analysis of critical infrastructures. *Reliab. Eng. Syst. Saf.* **2016**, *152*, 137–150. [CrossRef]
19. Tukamuhabwa, B.R.; Stevenson, M.; Busby, J.; Zorzini, M. Supply chain resilience: Definition, review and theoretical foundations for further study. *Int. J. Prod. Res.* **2015**, *53*, 5592–5623. [CrossRef]
20. Jain, V.; Kumar, S.; Soni, U.; Chandra, C. Supply chain resilience: Model development and empirical analysis. *Int. J. Prod. Res.* **2017**, *55*, 6779–6800. [CrossRef]
21. Wieland, A.; Wallenburg, C.M. The influence of relational competencies on supply chain resilience: A relational view. *Int. J. Phys. Distrib. Logist. Manag.* **2013**, *43*, 300–320. [CrossRef]
22. Ambulkar, S.; Blackhurst, J.; Grawe, S. Firm's resilience to supply chain disruptions: Scale development and empirical examination. *J. Oper. Manag.* **2015**, *33–34*, 111–122. [CrossRef]
23. Spiegler, V.L.M.; Naim, M.M.; Wikner, J. A control engineering approach to the assessment of supply chain resilience. *Int. J. Prod. Res.* **2012**, *50*, 6162–6187. [CrossRef]

24. Hosseini, S.; Al Khaled, A.; Sarder, M.D. A general framework for assessing system resilience using Bayesian networks: A case study of sulfuric acid manufacturer. *J. Manuf. Syst.* **2016**, *41*, 211–227. [CrossRef]
25. Xu, M.K.; Radhakrishnan, S.; Kamarthi, S.; Jin, X.N. Resiliency of Mutualistic Supplier-Manufacturer Networks. *Sci. Rep.* **2019**, *9*, 13559. [CrossRef] [PubMed]
26. Gu, X.; Jin, X.N.; Ni, J.; Koren, Y. Manufacturing System Design for Resilience. In Proceedings of the 25th CIRP Design Conference, Haifa, Israel, 2–4 March 2015; Elsevier Science Bv: Haifa, Israel, 2015; pp. 135–140.
27. Hu, Y.; Li, J.S.; Holloway, L.E. Resilient Control for Serial Manufacturing Networks with Advance Notice of Disruptions. *IEEE Trans. Syst. Man Cybern. Syst.* **2013**, *43*, 98–114. [CrossRef]
28. Qin, Y.T.; Zhao, L.P.; Yao, Y.Y. Dynamic quality characteristics modelling based on brittleness theory in complex manufacturing processes. *Int. J. Comput. Integr. Manuf.* **2011**, *24*, 915–926. [CrossRef]
29. Albino, V.; Garavelli, A. A methodology for the vulnerability analysis of just-in-time production systems. *Int. J. Prod. Econ.* **1995**, *41*, 71–80. [CrossRef]
30. Liu, W.Q.; Xu, L.Y.; Chen, Y.P.; Li, A.P. Structural Vulnerability Modeling and Evaluation of Manufacturing System Based on State Entropy. In Proceedings of the 51st CIRP Conference on Manufacturing Systems (CIRP CMS), Stockholm, Sweden, 16–18 May 2018; Elsevier Science Bv: Stockholm, Sweden, 2018; pp. 750–755.
31. Gao, G.B.; Wang, J.S.; Yue, W.H.; Ou, W.C. Structural-vulnerability assessment of reconfigurable manufacturing system based on universal generating function. *Reliab. Eng. Syst. Saf.* **2020**, *203*, 11. [CrossRef]
32. Wagner, S.M.; Neshat, N. Assessing the vulnerability of supply chains using graph theory. *Int. J. Prod. Econ.* **2010**, *126*, 121–129. [CrossRef]
33. Blackhurst, J.; Rungtusanatham, M.J.; Scheibe, K.; Ambulkar, S. Supply chain vulnerability assessment: A network based visualization and clustering analysis approach. *J. Purch. Supply Manag.* **2018**, *24*, 21–30. [CrossRef]
34. Wagner, S.M.; Neshat, N. A comparison of supply chain vulnerability indices for different categories of firms. *Int. J. Prod. Res.* **2012**, *50*, 2877–2891. [CrossRef]
35. Bogataj, D.; Bogataj, M. Measuring the supply chain risk and vulnerability in frequency space. *Int. J. Prod. Econ.* **2007**, *108*, 291–301. [CrossRef]
36. Chang, J.; Lu, H.B.; Shi, J. Stockout risk of production-inventory systems with compound Poisson demands. *Omega Int. J. Manage. Sci.* **2019**, *83*, 181–198. [CrossRef]
37. Li, J.S.; Blumenfeld, D.E.; Huang, N.J.; Alden, J.M. Throughput analysis of production systems: Recent advances and future topics. *Int. J. Prod. Res.* **2009**, *47*, 3823–3851. [CrossRef]
38. Li, J.; Meerkov, S.M.; Zhang, L. Production Systems Engineering: Review and Recent Developments. In *Handbook of Stochastic Models and Analysis of Manufacturing System Operations*; Smith, J.M., Tan, B., Eds.; Springer: New York, NY, USA, 2013; pp. 167–210.
39. Jia, Z.Y.; Zhang, L. Serial production lines with geometric machines and finite production runs: Performance analysis and system-theoretic properties. *Int. J. Prod. Res.* **2019**, *57*, 2247–2262. [CrossRef]
40. Meerkov, S.M.; Zhang, L. Transient behavior of serial production lines with Bernoulli machines. *IIE Trans.* **2008**, *40*, 297–312. [CrossRef]
41. Ju, F.; Li, J.S.; Horst, J.A. Transient Analysis of Serial Production Lines with Perishable Products: Bernoulli Reliability Model. *IEEE Trans. Autom. Control* **2017**, *62*, 694–707. [CrossRef]
42. Hou, Y.K.; Li, L.; Ge, Y.T.; Zhang, K.F.; Li, Y. A new modeling method for both transient and steady-state analyses of inhomogeneous assembly systems. *J. Manuf. Syst.* **2018**, *49*, 46–60. [CrossRef]
43. Ge, Y.T.; Li, L.; Wang, Y. Modeling of Bernoulli production line with the rework loop for transient and steady-state analysis. *J. Manuf. Syst.* **2017**, *44*, 22–41. [CrossRef]
44. Chen, J.C.; Jia, Z.Y.; Huang, L.Z.; Dai, Y.P. Transient Performance Evaluation of Flexible Production Lines with Two Bernoulli Machines and Dedicated Buffers. In Proceedings of the 16th IEEE International Conference on Automation Science and Engineering (CASE), Electr Network, Hong Kong, China, 20–21 August 2020; pp. 836–841.
45. Jia, Z.Y.; Huang, L.Z.; Chen, J.C.A. Order-Reduced Dynamic Decoupling Approach for Performance Evaluation of Multitype and Small-Batch-Based Serial Lines With Adjustments and Resets. *IEEE Syst. J.* **2021**, *15*, 3902–3912. [CrossRef]
46. Wang, M.Y.; Huang, H.X.; Li, J.S. Transient Analysis of Multiproduct Bernoulli Serial Lines with Setups. *IEEE Trans. Autom. Sci. Eng.* **2021**, *18*, 135–150. [CrossRef]
47. Chen, G.R.; Zhang, L.; Arinez, J.; Biller, S. Energy-Efficient Production Systems Through Schedule-Based Operations. *IEEE Trans. Autom. Sci. Eng.* **2013**, *10*, 27–37. [CrossRef]
48. Rahman, S. Theory of constraints. *Int. J. Oper. Prod. Manag.* **1998**, *18*, 336–355. [CrossRef]
49. Chang, Q.; Biller, S.; Xiao, G.X. Transient Analysis of Downtimes and Bottleneck Dynamics in Serial Manufacturing Systems. *J. Manuf. Sci. Eng. Trans. ASME* **2010**, *132*, 9. [CrossRef]